# The imaging of cervical spondylotic myeloradiculopathy

Susan Hesni[1] · David Baxter[2] · Asif Saifuddin[1]

## Abstract

This review provides a detailed description of the imaging features of cervical spondylotic myelopathy and radiculopathy, with a focus on MRI. Where relevant, we will outline grading systems of vertebral central canal and foraminal stenosis. Whilst post-operative appearances of the cervical spine are outside the scope of this paper, we will touch on imaging features recognised as predictors of clinical outcome and neurological recovery. This paper will serve as a reference for both radiologists and clinicians involved in the care of patients with cervical spondylotic myeloradiculopathy.

**Keywords** Cervical · Spondylotic · Spondylosis · Myelopathy · Degenerative · Disc · Disk · Disease · Spine · Arthritis · Myeloradiculopathy · Radiculopathy

## Introduction

Cervical spondylosis is a term encompassing various degenerative processes including intervertebral disc (IVD) degeneration, facet and uncinate joint arthropathy, and segmental instability that may lead to vertebral central canal and neural foraminal stenosis, thereby resulting in cervical spondylotic myelopathy (CSM) and radiculopathy respectively. The aim of this review is to provide a detailed overview of the imaging features of CSM and radiculopathy, with a particular focus on MRI.

## Standard imaging protocols

### Radiography

Radiography is limited in its assessment of cervical spondylosis as it only provides a 2-dimensional representation of a 3-dimensional structure. Alignment, disc height, and osteophytosis are adequately assessed, whilst lateral flexion and extension radiographs provide information regarding fused segments and instability. Nonetheless, radiographs are generally recommended as the first line investigation for patients with neck pain [1] and may aid in the identification of patients that should proceed to MRI. Dynamic radiographs may have a role in prediction of severity of degenerative disc disease by way of demonstrating segmental horizontal displacement [2].

### CT

CT is superior to MRI in the assessment of the bony causes of foraminal stenosis and in assessing bony anatomy for pre-operative planning [3]. MRI is usually used for detailed assessment of soft tissues, but CT scan can be a useful adjunct when metallic artefact reduces visibility on MRI. CT may also be utilised as the primary imaging modality when patient factors preclude MRI, such as claustrophobia or an inability to lie flat for prolonged periods. CT assessment of cervical IVD herniation offers moderate-to substantial inter-modality agreement with MRI, although it has a tendency to underestimate the AP extent of the herniated disc [4]. CT myelography, whilst providing excellent detail, has inherent risks and should be reserved for patients who cannot tolerate MRI [5]. The authors' standard protocol for pre-operative CT assessment of patients with CSM is included in this paper (Table 1 in the Appendix).

Waly et al. [6] undertook a systematic review of CT myelography parameters as predictors of outcome in patients with CSM. Five papers including 402 patients were

✉ Susan Hesni
  susan.hesni@nhs.net

1  Department of Radiology, Royal National Orthopaedic Hospital (RNOH), Stanmore, UK

2  Department of Surgery, Royal National Orthopaedic Hospital (RNOH), Stanmore, UK

reviewed, all being retrospective cohort studies. They found some evidence suggesting that patients with a pre-operative transverse spinal cord area > 30 mm$^2$ at the level of maximum compression had better post-operative recovery and outcome, but no studies investigated the correlation between pre-operative CT myelography parameters and severity of CSM. The authors concluded that patients with a greater spinal cord transverse area at the level of maximum compression on pre-operative CT myelography were more likely to have better post-operative neurological outcome.

## MRI

MRI is the preferred technique for the assessment of cervical spondylosis due to its excellent soft tissue detail and ability to assess the spinal cord. Standard MRI protocols include 2-planes, sagittal, and axial. Axial images comprise T1-weighted (T1W) and T2W sequences. Fast spin echo T2W images are excellent at delineating cord signal and are sensitive for detecting early IVD degeneration [7], whilst gradient echo sequences are superior for bony detail, such as the assessment of osteophytes. Care should be taken when assessing foraminal stenosis on gradient echo images, where it may be overestimated [8]. Intravenous gadolinium is not routinely used in spondylosis assessment but can provide information regarding the integrity of the spinal cord parenchyma and blood-spinal cord barrier [9].

## Cervical spinal anatomy and alignment

The cervical spine is the most mobile spinal segment, allowing flexion, extension, rotation, and lateral flexion [10]. It contains 7 vertebrae which gradually enlarge cranially to caudally. The atlantoaxial joint (AAJ) comprises C1 (atlas) and C2 (axis) vertebrae. The atlas has distinctive morphology with no proper vertebral body. The superior margins of the cervical vertebral bodies are concave when viewed from the frontal projection, convex when viewed laterally. At the lateral aspect of the superior surface is a bony projection known as the uncus [3], which articulates with the vertebral body above to form the uncovertebral joints (of Luschka) (Fig. 1). Like other joints, these can undergo degenerative change [11]. The cervical canal contains the cervical cord and is bounded anteriorly by the vertebral bodies, IVD, and posterior longitudinal ligament (PLL), which extends along the length of the spine. Posteriorly, the canal is bounded by the ligamentum flavum (LF) and laminae [12]. The cross-section of the cervical vertebral canal is triangular in shape [3].

The functional spinal unit (FSU) is the smallest motion segment of the spine formed by two adjacent vertebrae, an IVD, ligaments, and facet/uncovertebral joints. The biomechanics of the cervical FSU are similar to that of the remaining spine, with ~70% of axial load transmitted by the vertebral body and IVD and the remainder through the facet joints [13].

Cervical spinal curvature is best viewed on upright lateral radiographs [12]. Sagittal alignment is typically lordotic, although neutral and kyphotic curves may also be seen. Sagittal alignment can be measured using the cervical lordosis angle (the angle of intersection of two lines placed parallel to the inferior endplate of C2 and the inferior endplate of C7). With ageing, the degree of cervical lordosis tends to increase placing greater contact forces on the facet joints, whilst decreased lordosis results in increased contact forces on the vertebral bodies and IVDs [14]. The sagittal vertical axis (SVA) can also be calculated on lateral radiographs, representing the deviation of the C2 plumb-line from the posterior superior endplate of C7. Normal SVA is 16.8 mm ± 11.2 mm. When the SVA is > / = 40 mm, there is a strong correlation with disability [15]. In cervical spondylosis, there is a tendency towards straightening of the cervical lordosis, particularly in symptomatic patients, with a decreased range of motion from flexion to extension and greater horizontal displacement [16].

## Cervical spondylotic myelopathy

### Clinical features and epidemiology

Cervical spondylosis is extremely common. In adults over 60 years of age, degenerative changes are seen at one or more levels of the cervical spine in 96% of men and 89% of women [17]. In the United States, 13% of adults have experienced neck pain within the last 3 months [18]. After back pain, neck pain is the commonest musculoskeletal cause of primary care consultation worldwide [19], and CSM is the leading cause of spinal cord dysfunction in the older population [20]. Cervical spondylosis is rare in early life and is usually seen from the 3rd decade onwards [3]. However, a decreased incidence with age after 60 years suggests that ageing is not the only contributor [21]. Prevalence is increased in the setting of overuse, such as in athletes [22].

The symptoms of CSM are variable and depend upon the presence and severity of spinal cord and nerve root compression. Neck stiffness, neck pain, and upper limb weakness/numbness are characteristic and are usually progressive. However, spasticity is often the first symptom, manifest as reduced fine motor skills in the hands (difficulty texting on the phone or doing up shirt buttons), and increased frequency of falls [3, 23, 24]. In advanced cases, CSM may lead to quadriparesis and incontinence [25].

Surgery in cervical spondylosis is reserved for spinal cord or nerve root compression and may be combined with fusion to reduce the incidence of post-operative instability.

**Fig. 1** **a** Coronal T1W TSE and (**b**) axial PDW FSE MR images of the cervical spine of a 65-year-old female showing the uncus (arrows) bilaterally at the C5 level articulating with the vertebra above to form the C4-C5 uncovertebral joints. Note their location at the anterior margin of the intervertebral foramen
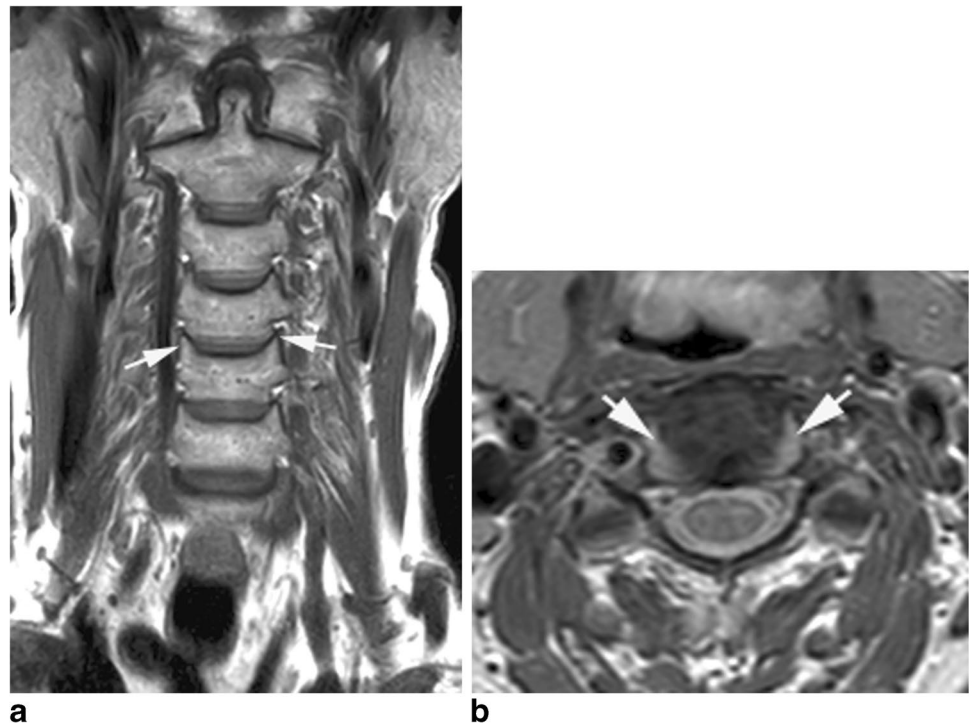


The surgical approach is influenced by several factors. If compression is predominantly from dorsal pathology such as a hypertrophied LF; then, most surgeons would perform a posterior decompression possibly combined with stabilisation using lateral mass screws. If the compressive pathology is predominantly ventral, such as an IVD bulge/protrusion or osteophyte; then, the usual approach would be anterior. As intervertebral discs degenerate, they lose volume and also height. This causes the annulus of the disc to buckle and protrude into the spinal canal or foramen causing neural compression. Surgery to restore the intervertebral height relieves this compression by causing the posterior longitudinal ligament to become tense and force the annulus into its original position. This process is known as ligamentotaxis. Placing a cage or artificial disc in the IVD space also restores foraminal height, indirectly decompressing the exiting nerve roots and thereby treating radicular symptoms. As well as the inherent risks of surgery, the loss of spinal movement that accompanies fusion may accelerate degeneration at adjacent spinal levels. Therefore, surgery should only be undertaken when conservative treatments have failed [3].

## Pathophysiology

CSM is the result of SCI in the presence of degenerative disease. Ellingson et al. [26] highlighted 2 forms of degenerative SCI, primary and secondary. Primary mechanical SCI is caused by compression, distraction, or shearing, for example, repetitive micro-trauma from cervical disc bulges during flexion and extension. Secondary SCI encompasses various mechanisms from ischaemia to free radical-mediated cell injury. In the degenerate spine, ventral compression can impair perfusion of the cord from the anterior sulcal arteries.

CSM may also be due to static and dynamic factors. Static factors include a congenitally stenotic canal, conditions such as Klippel-Feil syndrome (Fig. 2), ossification of the PLL (OPLL), diffuse idiopathic skeletal hyperostosis (DISH), and iatrogenic fusion. Dynamic factors include repetitive flexion or extension of the neck, the former compressing the cord against osteophytic spurs and disc bulges, and the latter leading to cord compression between the posterior vertebral body and LF [17]. Factors to be considered in the imaging assessment of patients with clinical suspicion of CSM include AP canal dimension, causes of reduced AP canal dimension, spinal alignment, and the status of the cervical cord (compression and T2W signal abnormality).

## Vertebral canal diameter

The AP canal dimension is easily measured on lateral radiographs and is a predictor of clinical symptoms. The measurement is taken from the posterior vertebral body cortex to the closest portion of the spinolaminar line at the pedicle level. Accuracy of radiographic measurement is limited by technical factors such as patient rotation and magnification, and measurements do not account for soft tissue structures (Fig. 3). Changes to cervical spine morphology and canal

**Fig. 2** A 39-year-old male with Klippel-Feil syndrome. (**a**) Sagittal and (**b**) axial T2W FSE MR images showing multilevel vertebral fusion (arrows) and a degenerate bulging C2-C3 disc resulting in cord compression and myelomalacia (arrowheads)
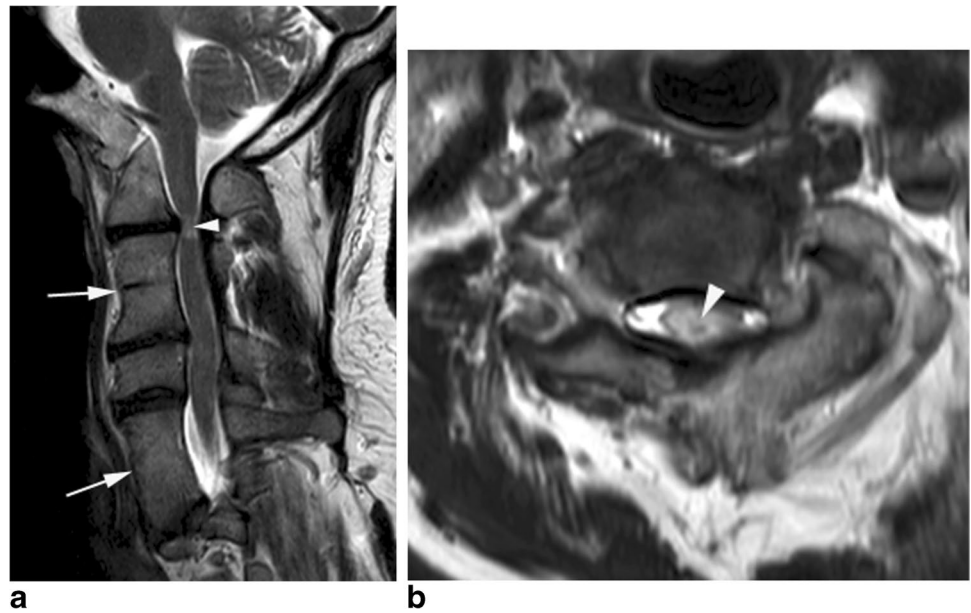


dimensions occur during movement, with widening in flexion and narrowing in extension, due to a combination of bony and soft tissue structures such as the IVD and LF. During flexion, the cord elongates and is located anteriorly within the canal where it can be impinged by disc bulges and osteophytes. During extension, the cord has a posterior location where it can be impinged by buckling of the LF [20, 27]. A narrower canal dimension in extension is compounded by shortening of the cord in extension, which increases cord thickness [8, 28, 29].
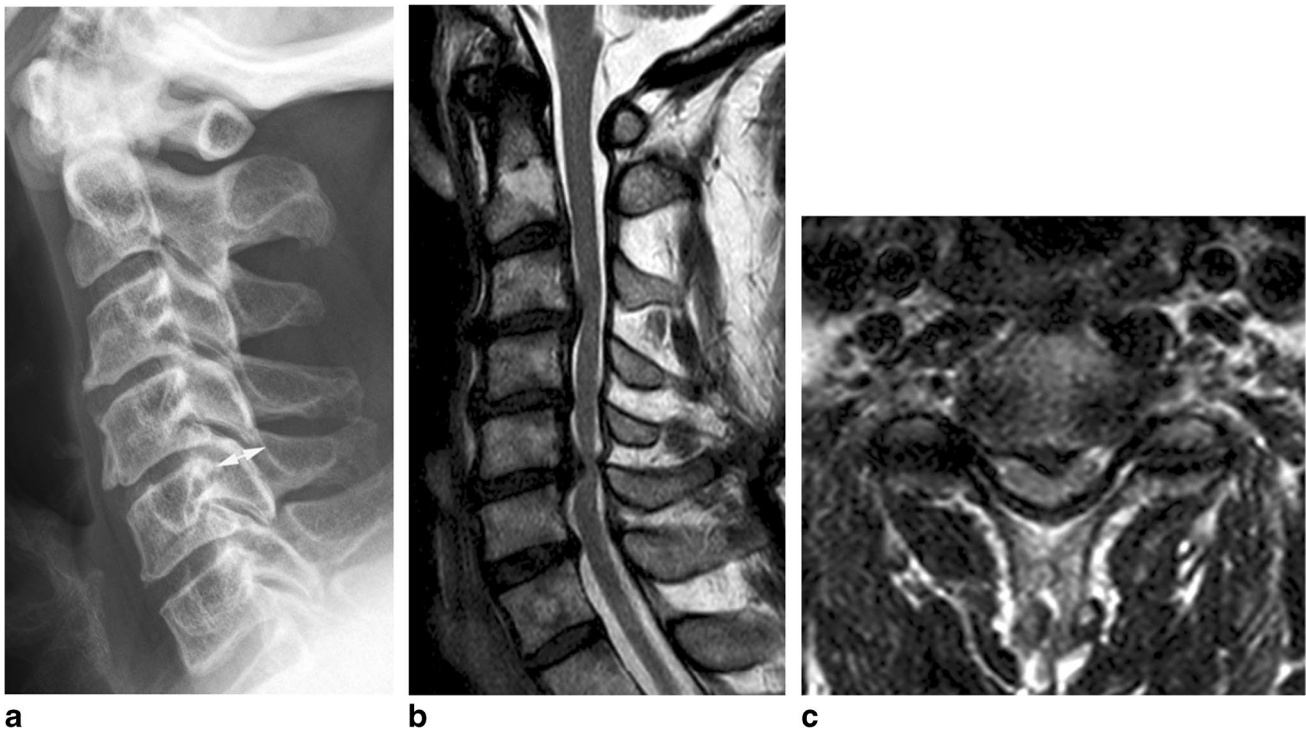


**Fig. 3** A 62-year-old male presenting with clinical features of CSM. (**a**) Lateral radiograph demonstrates a congenitally stenotic cervical canal, the AP dimension at C5 being 10 mm (double-headed arrow). The Pavlov ratio at C5 was 0.46. (**b**) Sagittal and (**c**) axial T2W FSE MR images showing multilevel degenerative disc disease with a prominent central protrusion ant C5-C6 reducing the AP canal dimension to 3 mm and resulting in severe cord compression

Zeng et al. [30] used upright kinetic MRI in the neutral, flexed, and extended positions to assess changes in AP canal dimension as well as changes to the morphology of disc bulges and LF thickness. They found that AP cervical canal dimensions significantly reduced in extension compared to flexion (flexion > neutral > extension) at the C3-C4 to C6-C7 levels, whilst LF diameter increased in extension (extension > neutral > flexion) (Fig. 4). Similarly, mean disc bulge diameter significantly increased in extension (Fig. 4). Changes in disc bulge and LF diameter were associated with significant reduction in AP canal dimension, particularly at C4-C5 and C5-6. AP canal diameters narrow from C2-C3 to C5-C6 then widen, being widest at C7-T1. In extension, C4-C5 and C5-C6 are narrowest [31].

A systematic review of the use of kinematic MRI in the assessment of spinal degeneration demonstrated significant reduction in the mobility of cervical segments in the presence of severe disc degeneration and in those with severe cord compression. Kinetic MRI was also found to be more specific and sensitive than conventional MRI in demonstrating objective imaging findings that relate to patient symptoms and improved disc herniation detection by 6–19% [32]. Similarly, a review by Xu et al. [33] suggested that dynamic supine cervical spine MRI detected occult or an increased degree of cord compression in ≥ 20% of patients and demonstrated an average narrowing of the cervical canal by 20% in comparison to the neutral position. The same authors have proposed a protocol for the use of dynamic flexion–extension MRI to determine the change in surgical plan in patients with CSM, the results of which are awaited [34].

Normal canal dimensions are highly variable. A study of 140 healthy volunteers found variation in AP canal dimension at C1 from 10.7–19.7 mm, at C3 from 9.4–17.2 mm, and at C6 from 9.2–16.8 mm [35]. Canal size decreases with age. In the 3rd decade, normal ranges are between 12.7–14.4 mm in men and 12.6–14.3 mm in women, whilst in the 8th decade measurements are 11–13.6 mm in men and 10.8–13.5 mm in women [12]. Spinal cross-sectional area is generally between 75 and 90 mm$^2$, peaking in the 3rd decade of life [12].

A radiographic AP canal dimension of < 10 mm may be associated with myelopathy, whilst dimensions between 13 and 17 mm are less strongly associated with myelopathy but are associated with symptomatic spondylosis. AP dimensions of > 17 mm are usually not associated with symptoms [5]. A diameter of 13 mm is an independent predictor of

**Fig. 4** An 84-year-old female presenting with clinical features of myelopathy. (**a**) Sagittal flexion, (**b**) sagittal extension, (**c**) axial flexion, and (**d**) axial extension T2W FSE MR images showing multi-level thickening of the ligamentum flavum in extension (arrows-**b**; arrowhead-**d**) and prominence of the C3-C4 disc bulge in extension (arrows **c** and **d**), the combined features resulting in cord compression
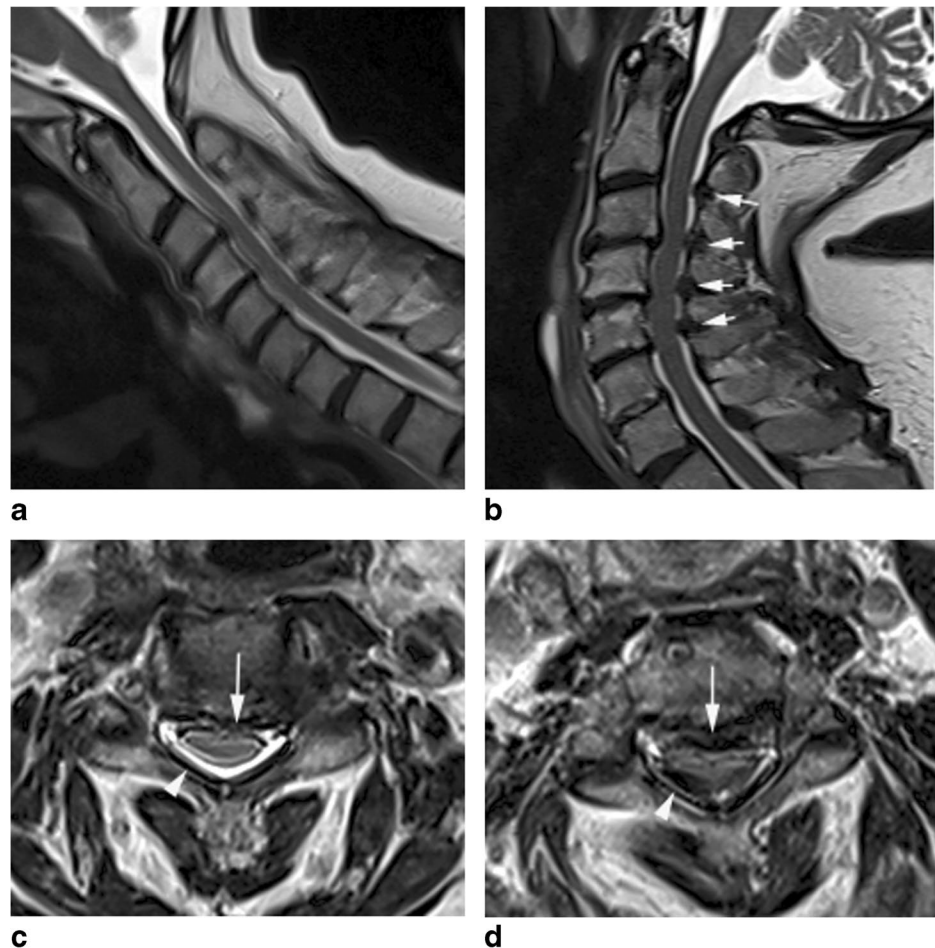
CSM [36]. A constitutionally narrow vertebral canal may be defined a sagittal canal AP dimension of < 13 mm (Fig. 3a) [37] and results in unique pathological and kinematic traits predisposing to degenerative disc disease, spinal canal stenosis, and myelopathy [5, 38]. Spinal cord occupation ratio (SCOR) of ≥ 70% can be used to diagnose congenital spinal stenosis and is associated with both earlier development of myelopathy and more severe impairment [39].

Alternative assessment of AP canal diameter includes the Pavlov ratio; the ratio between the vertebral canal and vertebral body depth is significantly lower in patients with CSM [40]. However, whilst correlation between Pavlov ratio and vertebral body:canal ratio on CT and vertebral body:CSF column ratio on MRI is good [41], correlation between Pavlov ratio and space available for the cord is poor [42] (Fig. 5). Congenital stenosis is defined on radiographs as a Pavlov ratio < 0.82 (Fig. 3a) [15].

On cross-sectional imaging, an occupation rate can be obtained by dividing the AP diameter of the spinal cord by that of the CSF-filled canal. This measurement has the advantage of accounting for differences in spinal cord size. Mean occupation rate at the C5 level is 58.3% ± 7%. An occupation rate of = / > 75% should be considered as congenital stenosis (Fig. 6) [12] and is associated with early development of symptoms [39, 43, 44].

When assessing spinal cord compression, the compression ratio (CR) is the most commonly used measurement, representing the ratio between the AP and transverse diameter of the cord at the region of greatest compression (Fig. 7). A CR of < 0.436 is associated with an unfavourable prognosis. This measurement is based on the premise that cord compression typically occurs as a result of AP diameter reduction and increase in lateral diameter. For this reason,

the measurement may be inappropriate in cases of circumferential compression [12, 45].

## Grading of central canal narrowing

Kang et al. [46] devised a grading system for the assessment of cervical canal stenosis on sagittal T2W images (Fig. 7). Grade 0 refers to the absence of canal stenosis. Grade 1 refers to near-complete obliteration of the subarachnoid space, including obliteration of the arbitrary subarachnoid space by > 50%, without cord deformity. Grade 2 refers to central canal stenosis with cord deformity, but in the absence of intrinsic cord signal abnormality. Grade 3 refers to T2W intrinsic cord signal abnormality at the compressed level. Inter-observer agreement was good–excellent (intra-class correlation coefficient (ICC) 0.716–0.802), whilst intra-observer agreement was excellent (ICC 0.768). This grading system was re-assessed by Waheed et al. [47] in order to determine the correlation with neurological symptoms. More than 1 neurological symptom in combination with MRI grade 2 or grade 3 stenosis was taken as positive evidence of cord compression secondary to canal stenosis. A strong agreement between neurological symptoms and the Kang grading system was demonstrated ($K = 0.81$ (95% CI 0.70–0.92), $p < 0.001$).

## Dynamic changes

### Cervical spondylolisthesis

Cervical spondylolisthesis refers to the slip of a vertebral body with respect to that below. Spondylolisthesis is measured as the distance between the posterior margins
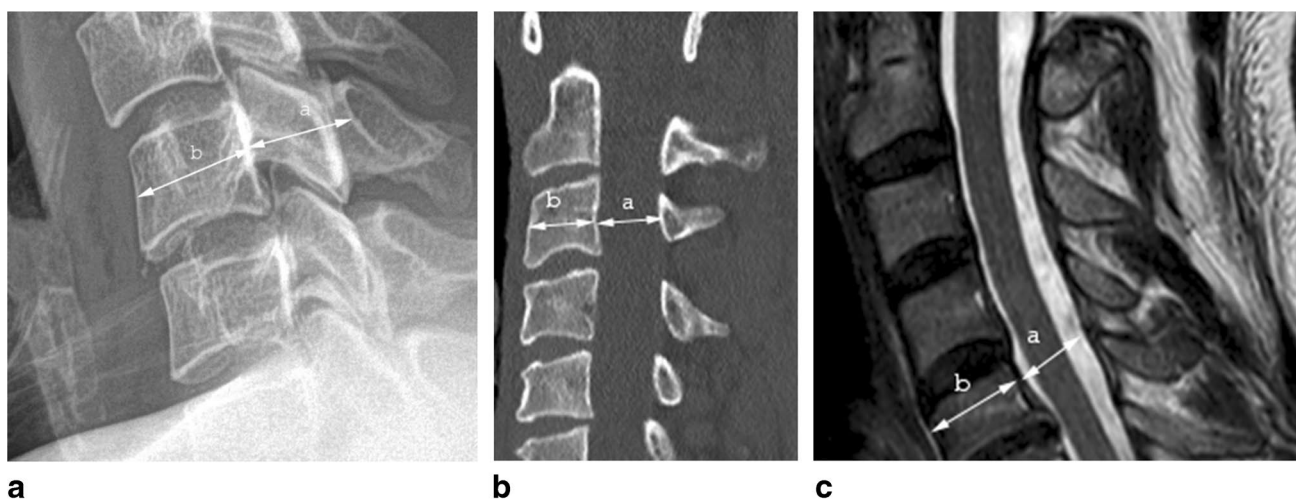


**Fig. 5** Radiological measurements. (**a**) Lateral radiograph demonstrating Pavlov ratio (a/b). (**b**) Sagittal CT demonstrating spinal canal to vertebral body ratio (a/b). (**c**) Sagittal MRI demonstrating CSF column to vertebral body ratio (a/b)

**Fig. 6** A 46-year-old female with neck pain referred to the jaw and shoulder. (**a**) Sagittal and (**b**) axial T2W FSE MR images showing multilevel degenerative disc disease. AP canal dimension at C5 was 9.3 mm and AP cord dimension 7.4 mm. Occupation ratio = 0.8 consistent with congenital canal stenosis
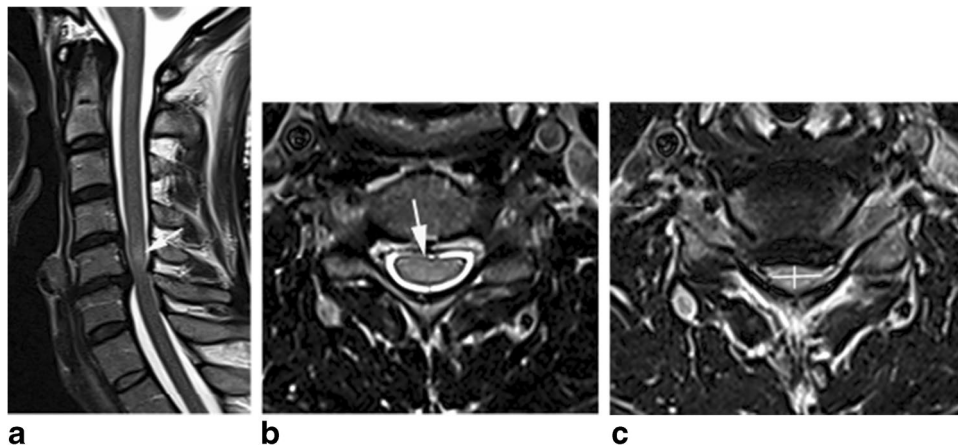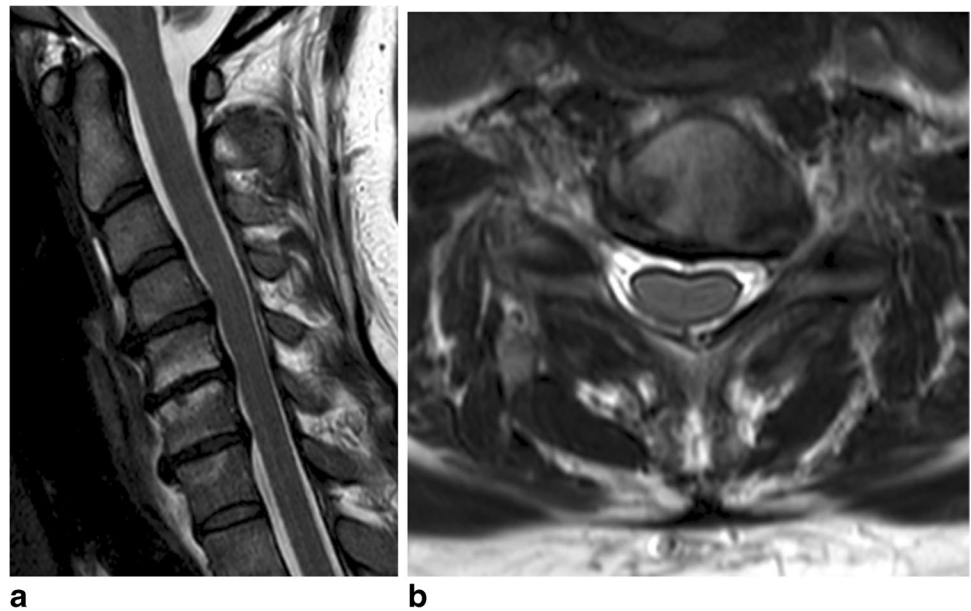


**Fig. 7** A 45-year-old male presenting with clinical features of CSM. (**a**) Sagittal and (**b**) axial T2W FSE MR images showing multilevel degenerative disc disease with a prominent diffuse disc bulge at C5-C6 compressing the cord. There is diffuse increased T2W cord SI (arrows-a,b) proximal to the site of compression. (**c**) The compression ratio was calculated at 0.45. Based on the Kang grading system for central canal stenosis, there is Grade 1 stenosis at C4-C5, Grade 3 stenosis at C5-C6 and Grade 0 stenosis at the remaining levels

of the affected vertebral body and the vertebral body below, with severe listhesis defined as > 3–3.5 mm of horizontal translation [12]. Spondylolisthesis is a marker of instability and occurs secondary to facet joint and IVD degeneration [48]. Disc degeneration and hypertrophic spurring can lead to cervical spine rigidity and ankylosis, placing increased stress on adjacent vertebral levels resulting in disc and ligamentous stretching, laxity, and slippage [23, 49]. This form of spondylolisthesis is a form of compensatory subluxation and is classified according to Dean et al. [50] as type 1 or 'adjacent' and is associated with facet joint osteoarthritis, erosions, joint remodelling, and subluxation [23]. Disc height at

the level of spondylolisthesis is typically relatively preserved [50]. In the less common type 2 spondylolisthesis, the slip occurs at the spondylotic segment where there is more advanced disc disease [50]. Spondylolisthesis is found in almost half of spondylotic patients on flexion–extension radiographs [23] and typically affects the upper cervical spine between C3-C5 [50, 51]. A recent study by Alvarez et al. [52] found that 22% of levels with spondylolisthesis identified on lateral flexion–extension radiographs are missed on neutral radiographs and that MRI misses 38% of cases.

Cervical spondylolisthesis is associated with CSM, with studies demonstrating cord compression and associated

T2W SI changes on MRI at the sites of spondylolisthesis (Fig. 8) [51]. Cervical spondylolisthesis results in conduction block on electrophysiological assessment, even in the presence of an apparently capacious canal [53]. Almost two-thirds of patients with cervical spondylolisthesis present with myelopathy or myeloradiculopathy [48]. Patients with a combination of spondylolisthesis and spondylosis are functionally worse at baseline presentation and have poorer post-operative outcomes following spinal decompression alone [54]. However, decompression combined with fusion can prevent spinal cord and nerve root compression, preventing deterioration and improving nerve root symptoms. Cervical spondylolisthesis may be dynamic and therefore underappreciated on static MRI imaging, with flexion–extension radiography or MRI offering additional benefit (see 'Dynamic Changes'). Up to 46% of patients with spondylolisthesis will demonstrate segmental instability on flexion–extension radiographs [48].

Anterior spondylolisthesis is seen in approximately 6% of the general population, most commonly at C4 [36], whilst retrolisthesis is seen in 13.2% of men and 8.9% of women, most often at C4 and C5. Both occur more frequently with increasing age [36], and severe listhesis may be seen in almost one-third of elderly patients [51]. Retrolisthesis is an independent predictor of CSM [36]. A recent systematic review and meta-analysis of spondylolisthesis in CSM showed that it is commoner in older patients and may be a predictor of advanced degeneration with worse baseline disability and post-operative outcomes [55].

In addition to spondylolisthesis, the presence of cervical lordosis or kyphosis is important to report, especially in cases going for surgery as it may affect the surgical approach [56, 57]. Anterior decompression and fusion is generally the preferred technique in those patients with only one or two compressive levels and a straightened or kyphotic spine as the anterior approach allows for better restoration of lordosis [56]. When the cervical spine is neutral or lordotic, a posterior approach such as laminectomy or laminoplasty may be preferred. Laminectomy and laminoplasty are not recommended in patients with cervical kyphosis as this may be worsened [56, 58]. A study by Shamji et al. [59] looking at the association of cervical spine alignment in neurological recovery found that greater improvement was seen in patients with preoperative cervical lordosis compared to those with cervical kyphosis. In those patients with cervical kyphosis, an anterior or combined approach was associated with improved post-operative outcomes. In addition to spinal curvature, the decision on surgical approach will take into a variety of factors including age, degree of pre-operative pain, number of levels involved, and presence of instability as well as the predominant site of pathology (anterior or posterior) [59].

### Ligamentum flavum buckling

LF buckling can reduce AP canal dimension and contribute to spinal cord compression. It occurs secondary to loss of IVD height and facet joint hypertrophy and may be influenced by genetic factors. The LF is thinnest centrally, and therefore, hypertrophy may be better appreciated on parasagittal slices [12].

Ossification of the LF has been described and can occur in the presence of OPLL, referred to as 'tandem ossification'. Calcification or ossification of the LF appears as low SI thickening on T1W and T2W images. It can be difficult to differentiate between hypertrophy



**Fig. 8** A 71-year-old female with symptoms of CSM. (**a**) Sagittal T2W FSE MR image and (**b**) sagittal CT MPR showing multi-level degenerative disc disease with C3-C4 spondylolisthesis (arrows) and myelomalacia (thin arrow-a). Hypointense soft tissue is demonstrated posterior to the dens (arrowhead-a). This is calcified on CT (arrowhead-b), consistent with pyrophosphate deposition in the transverse ligament
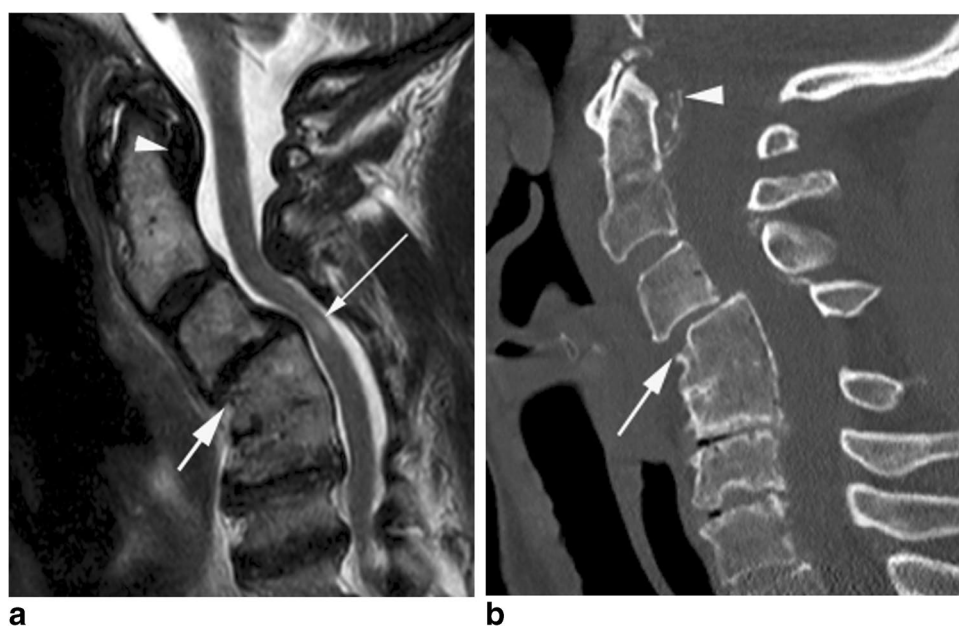
of the LF and calcification/ossification on MRI and in cases where the LF is contributing substantially to cord compression, CT can offer additional benefit (Fig. 9) [12]. Jeong et al. [60] looked at cervical LF thickness in 88 patients with canal stenosis and 87 controls, reporting a mean thickness of $1.41 \pm 0.24$ mm in normal subjects and $2.09 \pm 0.39$ mm in patients with canal stenosis. The authors determined a value of 1.71 mm to be the best cut-off (90.9% sensitivity, 90.8% specificity) as a predictor of cervical canal stenosis.

## Hypertrophy and ossification of the posterior longitudinal ligament

Both PLL hypertrophy and OPLL can occur and may appear similar, the former believed to be a precursor of ossification. Relative hyperintensity of the PLL on T1W images suggests hypertrophy, whilst the ligament is usually hypointense in OPLL [12]. In some cases, the normal PLL may be hard to distinguish from adjacent disc material, both appearing hypointense on standard T1 and T2W sequences [12]. Canal narrowing in OPLL may be severe enough to cause myelopathy [61].

OPLL most commonly occurs in the cervical spine and has an association with cervical spondylosis, occurring in up to 25% of spondylotic patients [62]. The pathogenesis of OPLL is unclear, but results from ectopic calcification. Both genetic and environmental factors have been implicated [61, 63], with segmental stress and reactive change to nucleus pulposus protrusion being implicated

[12]. Spinal instability is a common association [61, 62]. OPLL typically presents in the 5th–6th decades and affects men twice as commonly as women. There is an increased prevalence in the Japanese population (2 to 4% as compared with 0.01 to 2% in non-Asian populations) [64]. Symptom progression is usually more rapid when initial presentation occurs in the 4th decade or before [61].

OPLL may be diagnosed on radiographs, but is more accurately characterised with CT. MRI has a role in detecting spinal cord compression due to a reduction in AP canal dimension (Fig. 10). Sagittal images may be used to determine an 'occupancy ratio', which is defined as the ratio between the depth of the OPLL to the AP spinal canal dimension. A ratio of 30–60% predicts development of myelopathy, and when > 60% myelopathy is seen in 100% of cases. OPLL that occurs more laterally is also associated with a higher incidence of myelopathy [61]. OPLL is under-appreciated on MRI, with a reported sensitivity of only 49% [12].

The size, extent, and distribution of ossification can vary considerably. The most commonly used classification system for OPLL is that of the Japanese Ministry of Health, Labour and Welfare [61, 62] which categorises OPLL into 4 types: [1] continuous, a long lesion extending over several vertebral bodies (Fig. 10); [2] segmental, one or more separate lesions behind the vertebral bodies; [3] mixed, a combination of continuous and segmental types; and [4] circumscribed, mainly located posterior to a disc space (Fig. 11). This classification method has been found to have a concordance

**Fig. 9** An 88-year-old male with symptoms of CSM. (**a**) Sagittal T2W FSE MR image and (**b**) axial CT showing multilevel degenerative disc disease with multi-level thickening of the ligamentum flavum (arrows-a) and myelomalacia at C3-C4 (thin harrow). The ligamentum flavum is ossified on CT (arrow-b)
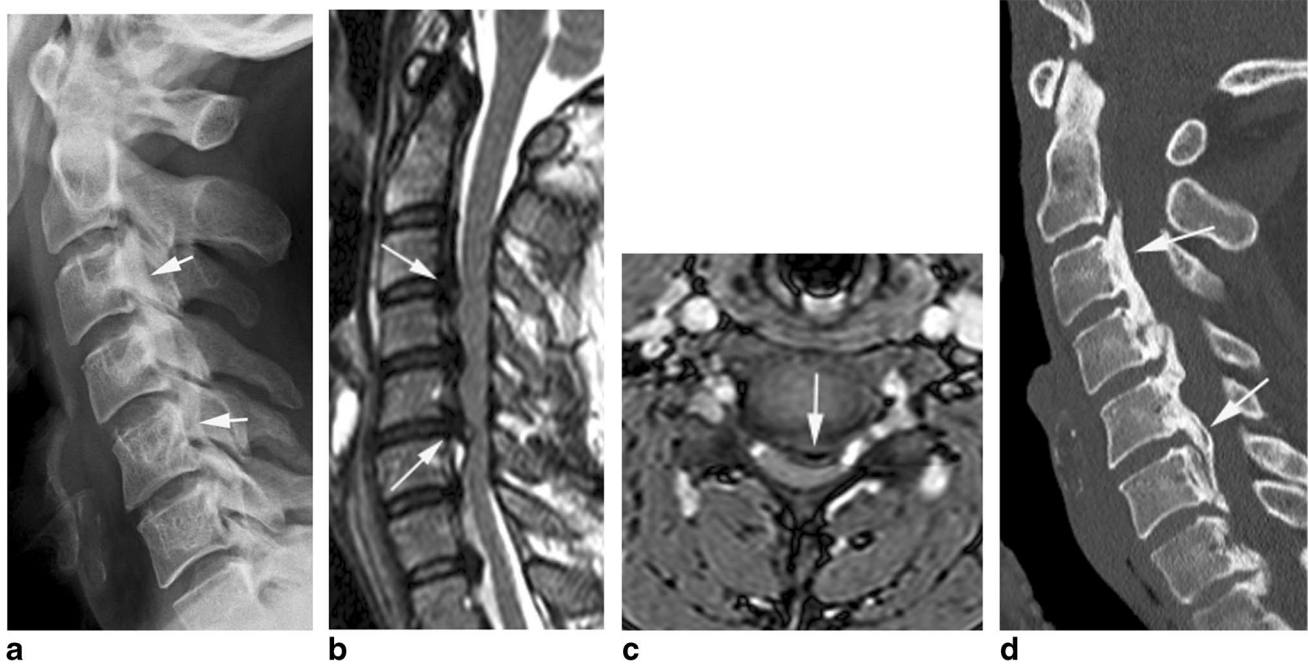
**a**    **b**
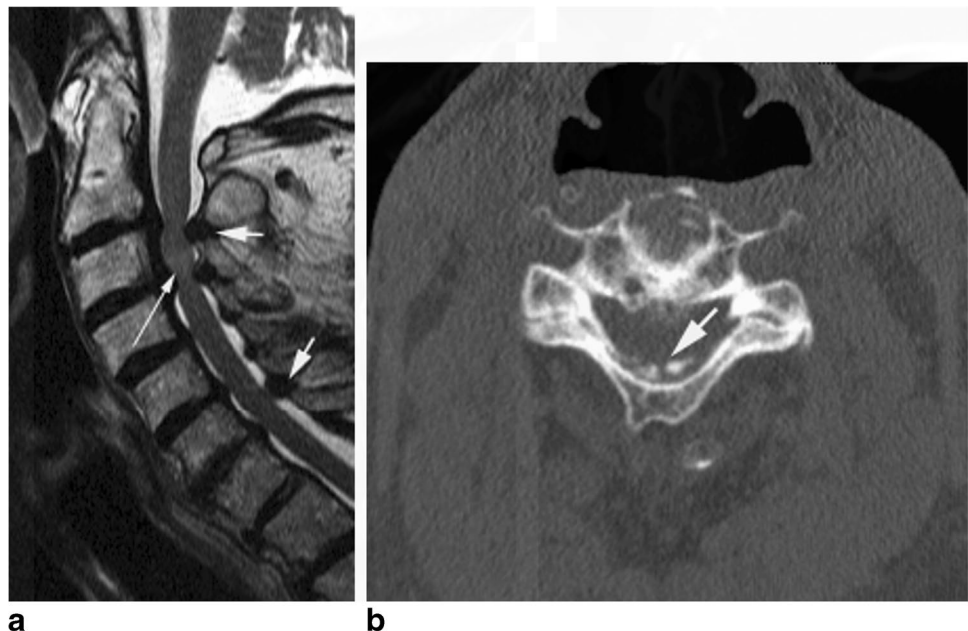
**Fig. 10** A 40-year-old male presenting with clinical features of CSM. (**a**) Lateral radiograph demonstrates extensive ossification of the PLL (arrows). (**b**) Sagittal and (**c**) axial T2W FSE MR images showing multi-level OPLL manifest by lobular hypointense thicken-ing (arrows) between the vertebral bodies and the compressed spinal cord. The occupancy ratio at C5-C6 was calculated at 54%. (**d**) Sagittal CT MPR confirms dense ossification over the posterior vertebrae from C2-C3 to C7-T1 (arrows) consistent with type 1 OPLL

**Fig. 11** A 51-year-old male presenting with clinical features of myelopathy. (**a**) Sagittal T1W TSE and (**b**) T2W FSE MR images showing multilevel OPLL manifest by lobular hypointense thickening (arrows) located predominantly at the disc spaces. (**c**) Sagittal CT MPR confirms dense ossifica-tion at these locations (arrows) consistent with type 4 OPLL
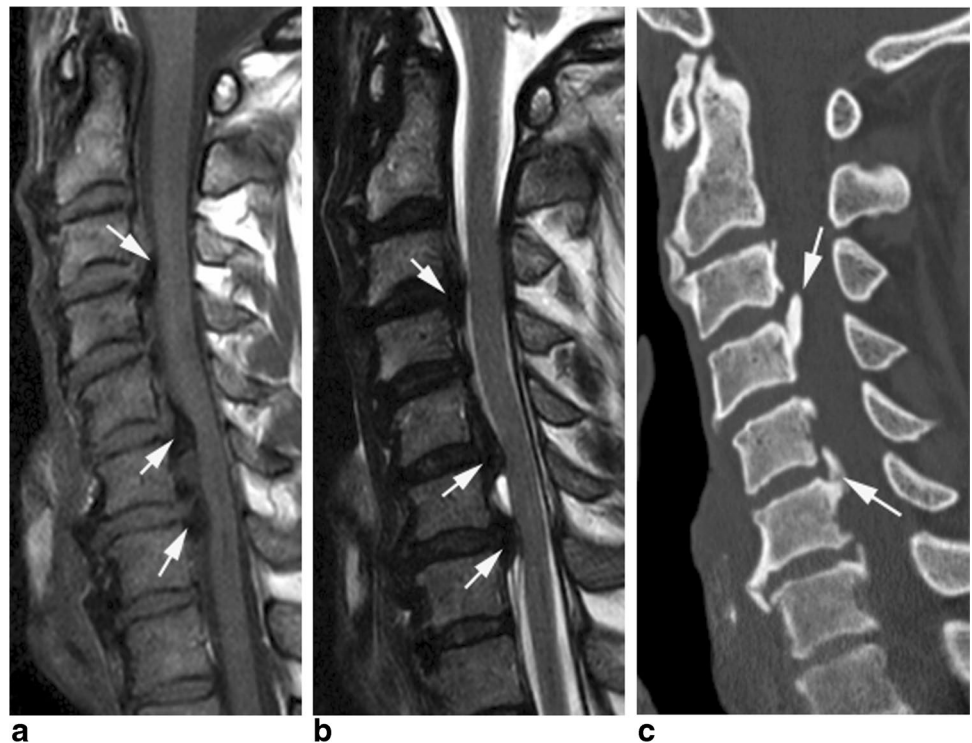
rate between X-ray and CT of 60% [65]. The most effective imaging method for characterisation of OPLL is 2D or 3D CT [62].

### Ossification of the nuchal ligament

The nuchal ligament is a triangular fibrous membrane extending from the occipital protuberance to the spinous process of C7. It maintains cervical lordosis and limits cervical movement. Ossification of the nuchal ligament (ONL) is associated with the development of instability and therefore accelerated osteophyte formation and IVD degeneration. Wang et al. [66] reviewed the relationship between ONL and pathological changes in the cervical spine in patients with spondylosis, finding that location of ONL corresponds to the most stenotic level of the spinal canal. Location of ONL also correlates with the level of IVD degeneration and osteophyte formation. The authors suggested that ONL corresponds to instability-related spine changes in cervical spondylosis.

## Cervical radiculopathy

Cervical radiculopathy refers to the symptomatic compression of nerve roots typically by herniated disc material, facet joint hypertrophy, or uncinate joint osteophytes. It typically results in neck and arm pain, numbness, and motor and/or sensory deficits [67, 68]. In 80% of patients, either the C6 or C7 nerve root is involved [69], and the condition typically affects those in the 4th–5th decades with an annual incidence of 107.3 per 100,000 in men and 67.5 per 100,000 in women [70]. The course of degenerative cervical radiculopathy is favourable, with the majority of patients responding well to conservative measures [67, 69, 71]. MRI is the imaging modality of choice, but the concordance between clinical level, electromyography, and MRI is only 50–70% [72]. The orientation of the cervical exit foramen can make assessment of stenosis challenging, and for this reason, non-standard techniques such as oblique sagittal sequences have been proposed, although the added benefit is unclear [73, 74]. Similarly, the addition of oblique sagittal and 3D-CT has been suggested, although this remains non-standard practise [75, 76].

### Cervical nerve root anatomy

The cervical nerve roots represent a confluence of the ventral and dorsal roots, the latter being 3 times larger than the former. The posterior root contains the spinal ganglion, which contains the cell bodies of sensory neurons. This spinal ganglion is located between the vertebral artery anteriorly and facet joint posteriorly. On a parasagittal slice, when bordered by the posterior vertebral body

cortex anteriorly and the pedicles above and below, the cervical nerve root is found either at the same level or inferior to the IVD [77]. The course of the cervical nerve roots as they pass from intradural to extra-vertebral can be divided into 3 segments. At the medial aspect of the exit foramen, the nerve roots are in a region equivalent to the lateral recess of the lumbar spine. Here, there is a relatively large amount of perineural space. Laterally, the nerve rests within a convexity of the transverse process with the vertebral artery anteriorly (Fig. 12), an important relation to note during cervical nerve root injection. In between these two areas is a narrow region bordered by the uncus anteriorly and facet joint posteriorly which forms the intervertebral foramen (IVF). The anatomical relations of the IVF mean that lateral disc bulges/protrusions (Fig. 13), uncinated joint osteophytes (Fig. 14), and facet joint hypertrophy (Fig. 15) can all lead to foraminal narrowing and cervical nerve root compression [3]. Radicular symptoms may cause diagnostic difficulty, leading to shoulder or chest pain in the case of C5 and C6 radiculopathy respectively. Therefore, it is important to consider lower cervical nerve root compression as a differential diagnosis in cases of shoulder or chest pain.

### Grading of cervical exit foraminal stenosis

In 2013, Park et al. [78] formulated an MRI grading system for cervical foraminal stenosis based on oblique sagittal images which comprised 4 grades. Grade 0 refers to absence of foraminal stenosis. Grade 1 refers to mild foraminal stenosis with partial (< 50% root circumference) peri-neural fat obliteration and no morphological change of the nerve root. Grade 2 refers to moderate (> 50% of root circumference) foraminal stenosis resulting in nearly complete peri-neural fat obliteration without morphological nerve root changes. Grade 3 refers to severe foraminal stenosis with nerve root collapse or morphological changes. They found a near-perfect level of both inter- and intra-observer agreement and later went on to assess the correlation with clinical findings [79]. They found that grades 2 and 3 were associated with positive neurological manifestations defined as > 1 positive neurological clinical symptom combined with > 1 positive neurological sign, and that the grading system successfully predicted positive neurological manifestations at these grades. However, this grading system was limited by its use of non-standard sagittal oblique sequences and grading using axial images is more suitable in standard practise. In 2015, Kim et al. [80] published a new grading system for cervical foraminal stenosis based on axial T2W images: grade 0, absence of neural foraminal stenosis with the narrowest width of the neural foramen greater than the width of the extra-foraminal nerve root (EFNR).

**Fig. 12** A 37-year-old male imaged for neck pain. (**a**) Sagittal and (**b**) axial T2W FSE MR images showing the dorsal root ganglion (arrows) located between the vertebral artery (thin arrow) and the facet joint (arrowhead)
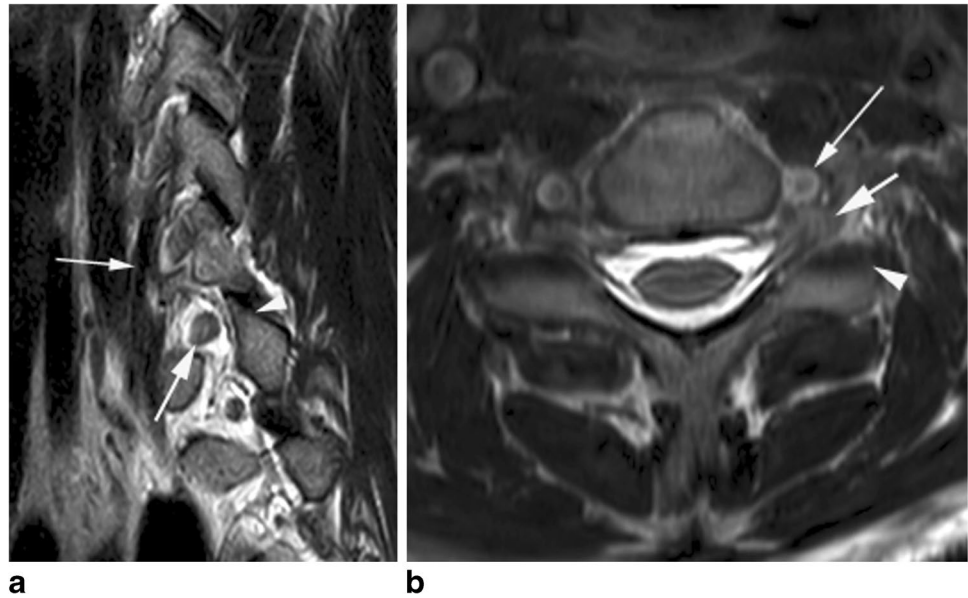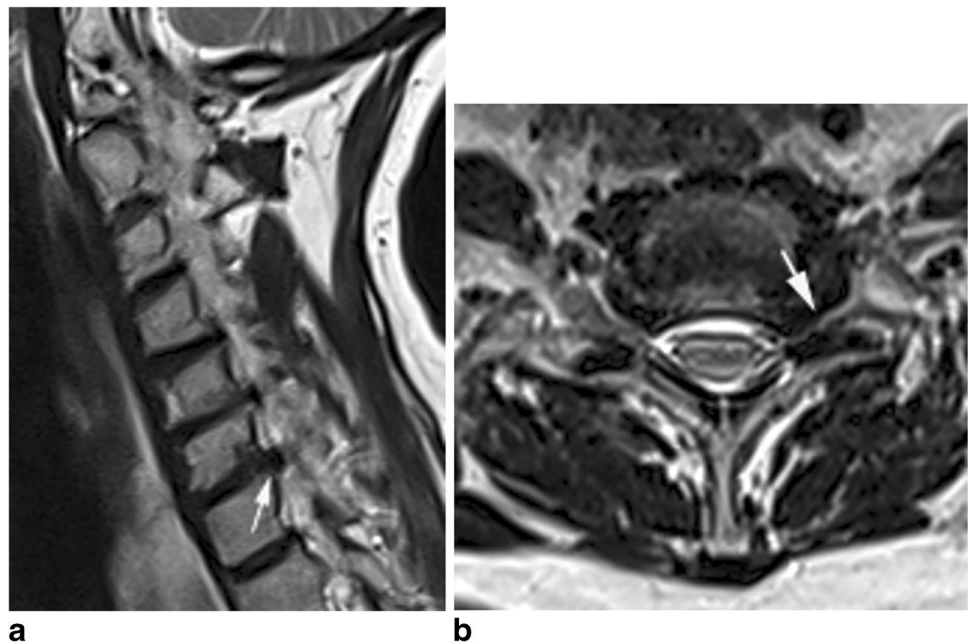


**Fig. 13** A 59-year-old female imaged for neck and bilateral arm pain, L > R. (**a**) Sagittal and (**b**) axial T2W FSE MR images showing a left C6-C7 intra-foraminal disc protrusion (arrows) resulting in grade 2 foraminal stenosis based on the Kim grading system, with compression of the left C7 nerve root. Grade 1 stenosis is present on the right side



Grade 1, a neural foramen with the narrowest width the same or less than (but > 50% of) the width of the EFNR (Fig. 13b). Grade 2, neural foramen with the narrowest width < 50% of the width of the EFNR (Figs. 13b and 14b). Inter-observer agreement ranged from fair-to-good (ICC 0.68–0.73) whilst intra-observer agreement was excellent (ICC 0.83–0.85). The authors concluded that

this MRI grading system showed sufficient inter- and intra-observer agreement to serve as a reliable method for evaluating cervical foraminal stenosis.

In 2016, Lee et al. [81] compared the grading systems of Park et al. [78] and Kim et al. [80]. The authors took > 1 neurologically relevant clinical symptom and > 1 neurologically relevant clinical sign as a positive manifestation
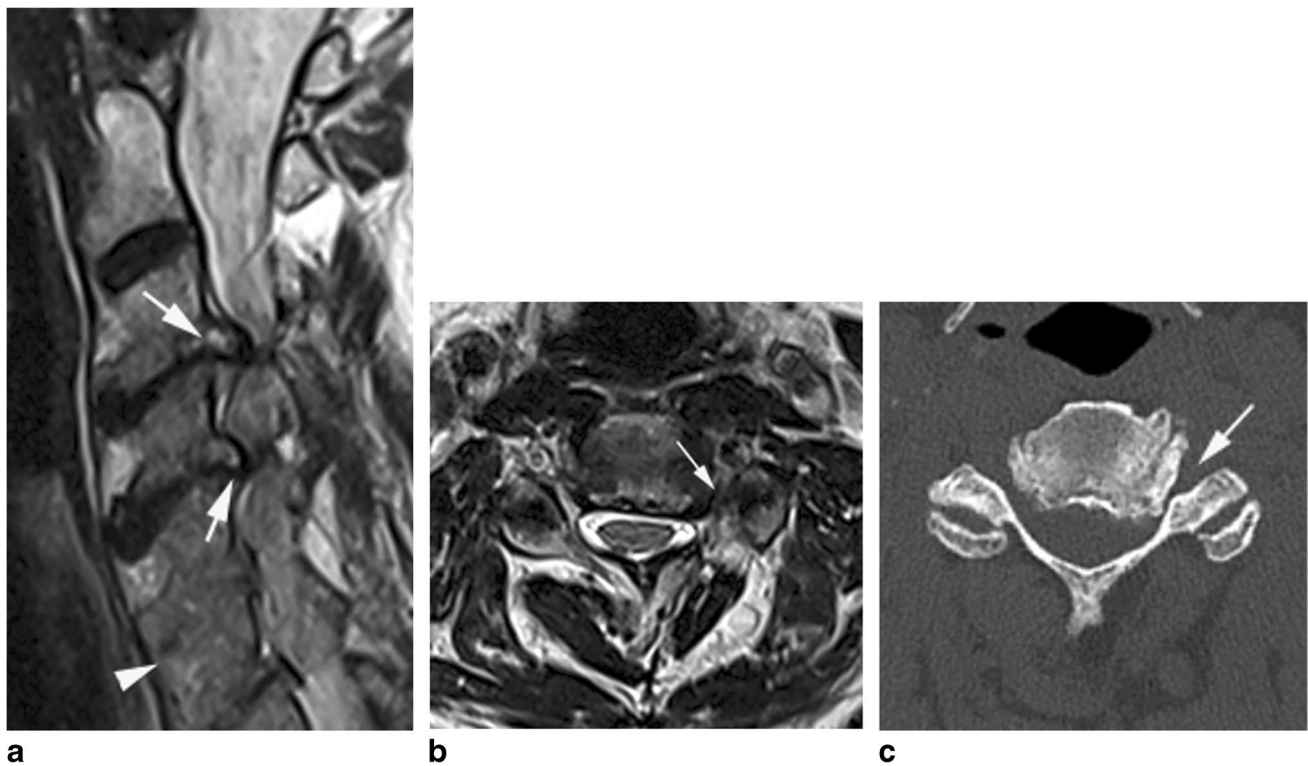
**Fig. 14** A 66-year-old male with worsening bilateral arm and hand symptoms following previous C5-C6 ACDF. (**a**) Sagittal and (**b**) axial T2W FSE MR images showing left C3-C4 uncinate joint osteophytes (longer arrow-a, arrow-b) resulting in grade 2 foraminal stenosis based on the Kim grading system, with compression of the left C4 nerve root. Similar changes are seen at C4-C5 (shorter arrow-a). Note also C5-C6 fusion (arrowhead-a). (**c**) Axial CT at the C3-C4 level confirms the bony foraminal compromise (arrow)
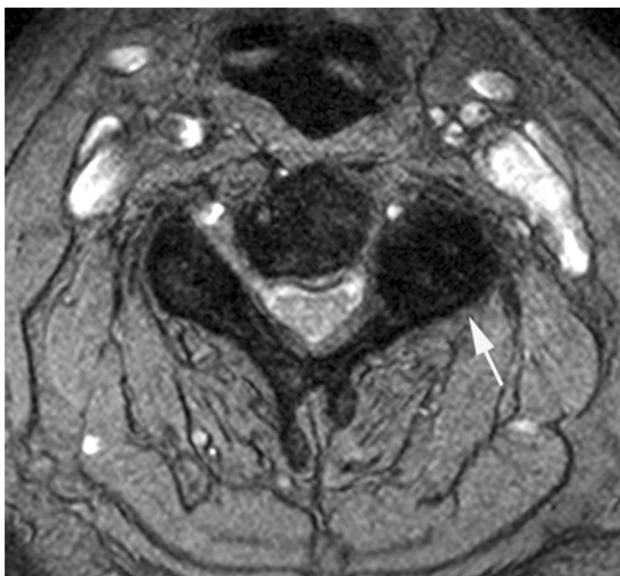


**Fig. 15** A 77-year-old male with bilateral arm. Axial T2*W GrE MR image showing left C3-C4 hypertrophic facet joint osteoarthritis (arrow) resulting in grade 2 foraminal stenosis based on the Kim grading system, with left C4 root compression

of foraminal stenosis, finding that both grading systems had relatively high correlation between stenosis grade and clinical manifestations ($R = 0.714$–$0.764$), concluding that both systems were reliable and reproducible. Meacock et al. [82] undertook a systematic review of existing radiological grading systems for cervical foraminal stenosis. The grading systems described by Kim et al. [80] and Park et al. [78] were considered to be the most robust, but the authors noted that the Park grading system relied on non-standard MRI sequences.

Engel et al. [83] evaluated the use of susceptibility-weighted MRI (SW-MRI) in the assessment of cervical foraminal stenosis. The authors compared SW-MRI with conventional T1W and T2W sequences and used CT as a reference standard. The study included 81 patients with 93 osteophytes and 114 disc herniations. SW-MRI had a significantly higher rate of detection ($p < 0.05$) and demonstrated high levels of sensitivity (96.6%) and specificity (99.5%) in the identification of foraminal stenosis (Fig. 16). This compares to sensitivity and specificity levels of 43.1% and 100% for T1W images and 65.5% and 99.1% for T2W images. Inter-observer agreement was
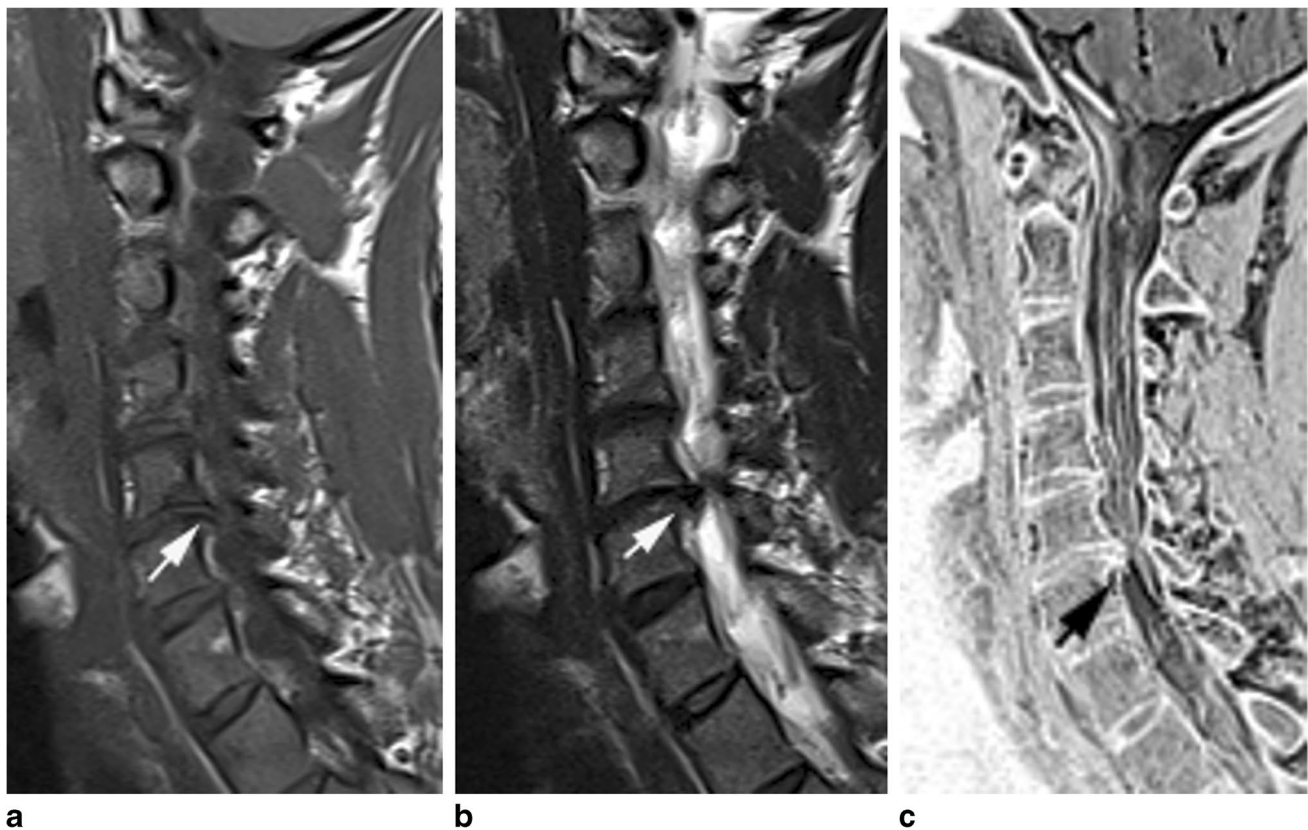
**Fig. 16** A 45-year-old male presenting with signs of CSM. (**a**) Sagittal T1W TSE, (**b**) T2W FSE, and (**c**) inverted susceptibility weighted MR images showing a right C5-C6 posterolateral osteophytes (arrows) which are optimally visualised on the susceptibility weighted sequence

highest for SW-MRI and severity scores were comparable to CT. The authors noted that T1W and T2W images tended to underestimate the degree of stenosis. Therefore, SW-MRI may offer a reliable and more sensitive way of assessing osseous foraminal stenosis precluding the need for CT and may be especially useful in young patients in whom radiation reduction is of particular importance.

Zero echo time MRI (ZTE-MRI) is a technique which can optimise the MRI assessment of cortical bone and has been described for the assessment of cervical foraminal stenosis. A substantial agreement was demonstrated between ZTE-MRI and CT for the grading of foraminal stenosis [84].

CT-guided nerve root blocks also have the ability to act as a diagnostic adjunct to MRI in confirming nerve root compression as the source of pain [85, 86].

## Cervical osteophytes and the 'osteophyte disc-bar complex'

Cervical spine degeneration leads to bony changes such as vertebral body flattening, increase in AP vertebral diameter, and osteophytosis as a response to abnormal biomechanical stresses [87]. As in IVD disease, the C5-C6 level is most frequently affected. Cervical osteophytosis may be severe enough to cause dysphagia [88].

The term 'osteophyte disc-bar complex' is widely used in the reporting of cervical spine MRI. However, Yousem [89] stated that this term may be misleading, as in many cases disc protrusions and osteophytes do not co-exist. The use of gradient echo sequences can assist in the differentiation of disc protrusions, which will appear relatively hyperintense on T2W compared to osteophytes which appear hypointense. He went on to state that surgeons are keen to differentiate between disc and osteophyte as it affects the proposed surgical procedure, and in the case of an isolated disc protrusion, there is an option of conservative treatment allowing the disc to resorb whereas osteophytes do not regress. If the disease is predominantly osteophyte-based, a more complex procedure with anterior drilling may be required. Conversely, Ross [90] claimed that the term is both widely accepted and appropriate, arguing that on routine MRI, low SI material may comprise a mixture
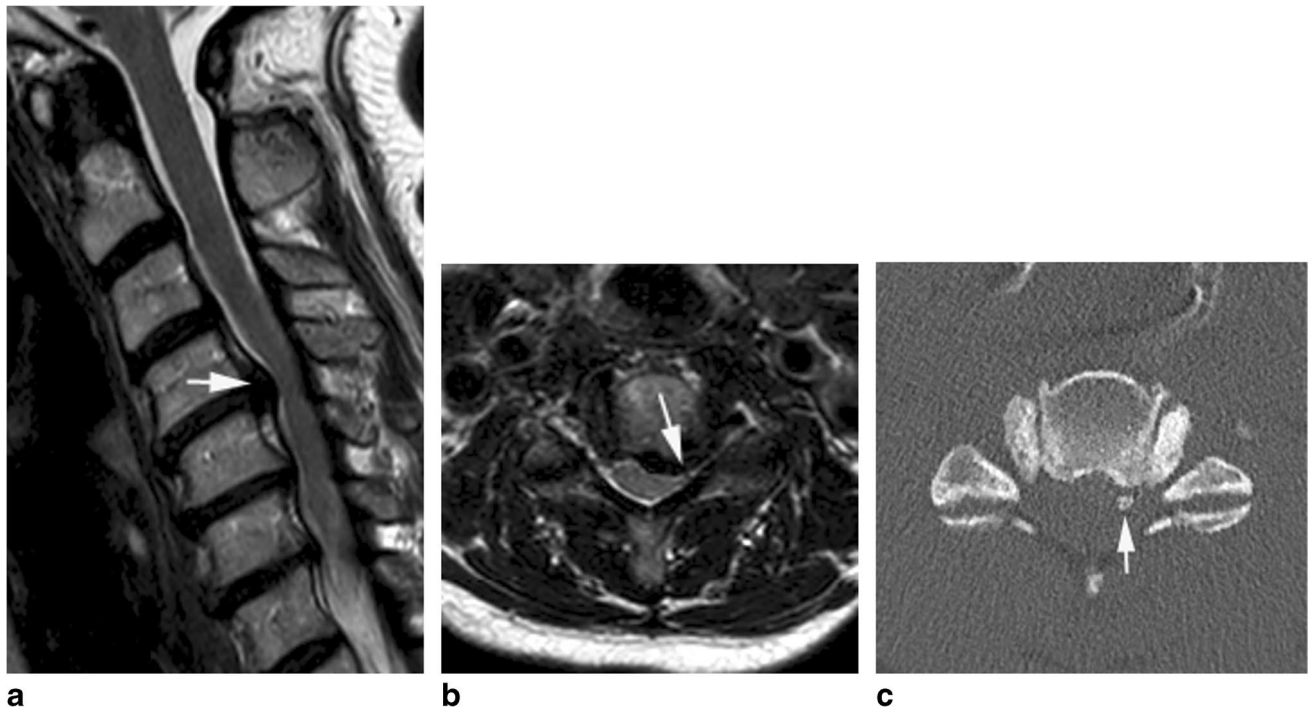
**Fig. 17** A 59-year-old female with neck pain and radiation to the left shoulder. (**a**) Sagittal and (**b**) axial T2W FSE MR images show a hypointense left C4-C5 disc protrusion resulting in lateral recess and foraminal stenosis with left C5 root compression. (**c**) Axial CT at the C4-C5 level confirms calcification within the protrusion (arrow)

of osteophyte, disc, calcification, and cartilage and that detailed assessment is often made difficult by patient cooperation, slice thickness, and magnet strength. Ross went on to state that CT should be obtained in cases where more detailed information is required regarding the presence of calcification (Fig. 17).

Sengupta et al. [91] assessed the ability of MRI to ascertain the presence of, and differentiate between soft cervical disc protrusion and osteophytes based on T2W SI characteristics, disc protrusions being relatively hyperintense (Fig. 18) whilst osteophytes were hypointense. Intra-observer agreement was poor for classification into hard material, soft material, or both. Intra-observer agreement for the presence or absence of hard disc material was moderate-to-good (Kappa = 0.6), and there was fair-to-moderate inter-observer agreement (Kappa = 0.4). MRI tended to overestimate the presence of hard disc, with a sensitivity of 87% but specificity of only 44%. Incidence of hard discs increased in the elderly, seen in 76% of those aged 50 years or more. The authors found no significant association between the presence of myelopathy or radiculopathy and the finding of hard or soft disc at operation. Similarly, Bender et al. [92] evaluated susceptibility-weighted magnetic resonance imaging (SW-MRI) for the differentiation of

osteophytes and disc herniations compared to conventional MRI sequences. Most osteophytes and disc herniations could be identified and differentiated on SW-MRI with a sensitivity of 98.9% and specificity of 99.1% for the identification of osteophytes (Fig. 16), whilst conventional T1W and T2W MRI sequences achieved a sensitivity and specificity of 68.6% and 86.5%, respectively. SW-MRI also showed a strong correlation with CT and radiography for assessing the size of osteophytes. The regression of disc-osteophyte complexes following cervical laminectomy and fusion suggests that this likely provides another mechanism of spinal cord decompression following surgery [93].

Approximately 40% of cervical disc herniations regress spontaneously [94]. Three hypotheses have been proposed for spontaneous regression: retraction of the disc, gradual dehydration and shrinkage, and inflammatory reaction causing neovascularity, enzymatic degradation, and phagocytosis [95]. Paracentral and foraminal disc herniations regress more frequently than central disc herniations and migrated and sequestered discs are more likely to regress when compared to simple disc protrusions [94–97] (Fig. 18). Contact with the epidural space appears to be an important determinant in disc regression (96, 98). When disc fragments contact the epidural space, there is an inflammatory response
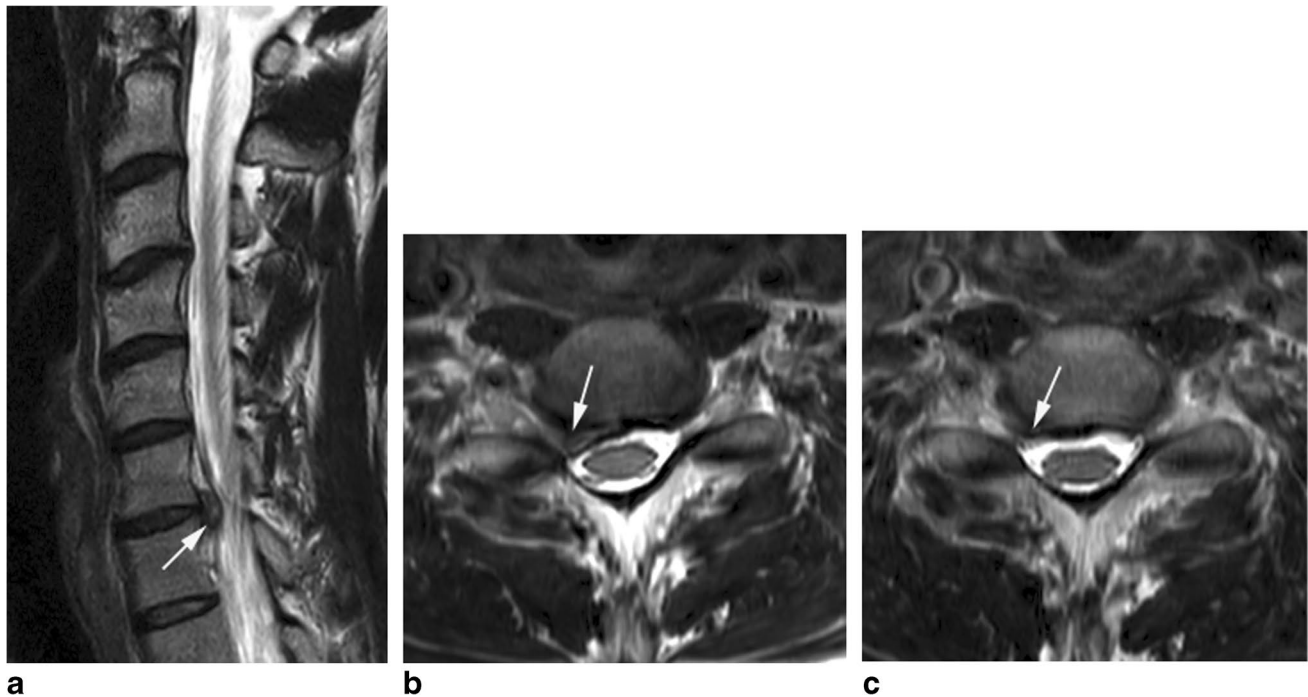
**Fig. 18** A 36-year-old male with neck pain and radiation to the right arm in the C7 distribution. (**a**) Sagittal and (**b**) axial T2W FSE MR images show a relatively hyperintense right C6-C7 disc protrusion (arrows-a and b) resulting in right C7 root compression. (**c**) Axial T2W FSE MR image obtained 6 months later shows almost complete resolution of the protrusion (arrow)

seen histologically as granulation tissue and neovascularity [96, 98]. This response is more prominent in transligamentous versus subligamentous extruded discs and may be the reason for quicker resorption [94, 96]. In the lumbar spine, this neovascularity has been well demonstrated on contrast-enhanced MRI and the thickness of this rim enhancement is a positive predictor of spontaneous regression (99). Average time from presentation to spontaneous regression of cervical discs is 9.15 months [97], although partial regression has been seen as early as 3 weeks [100]. A large study of 70 patients looking only at sequestered discs found a mean regression time of 5.7 months [96].

### Cervical cord changes

MRI findings of CSM include intramedullary T2W hyperintensity (Figs. 2, 8 and 9) with or without reduced T1W signal intensity (SI), which reflects increased water content. Such SI abnormality may be seen in up to 85% of patients with CSM [12]. However, incidental T2W hyperintensity may be encountered in 2.3% of asymptomatic subjects [12]. In the context of CSM, the significance of such intramedullary SI abnormality is contentious [17], in particular whether it relates to irreversible SCI or if there is potential for recovery is not fully understood. The potential morbidity of cervical decompression procedures has led to interest in determining which patients will benefit most from surgical intervention. A large systematic review by Mummaneni et al. [101] looked at clinical outcomes following surgical intervention and highlighted key imaging features which conveyed a poor prognosis. These included multilevel T2W hyperintensity and combined T1W focal hypointensity and T2W focal hyperintensity and cord atrophy. A meta-analysis undertaken by Chen et al. [102] looked at pre-operative MRI features in 650 CSM patients with or without intramedullary T1W and T2W SI abnormality, finding that surgical outcomes were significantly poorer in the presence of intramedullary signal changes, particularly when these were multi-segmental, well-defined, and with corresponding T1W SI change. When intramedullary signal change was focal or faint, outcomes were similar to those patients without intramedullary signal change. Similar findings have been found by other authors [103, 104, 105].
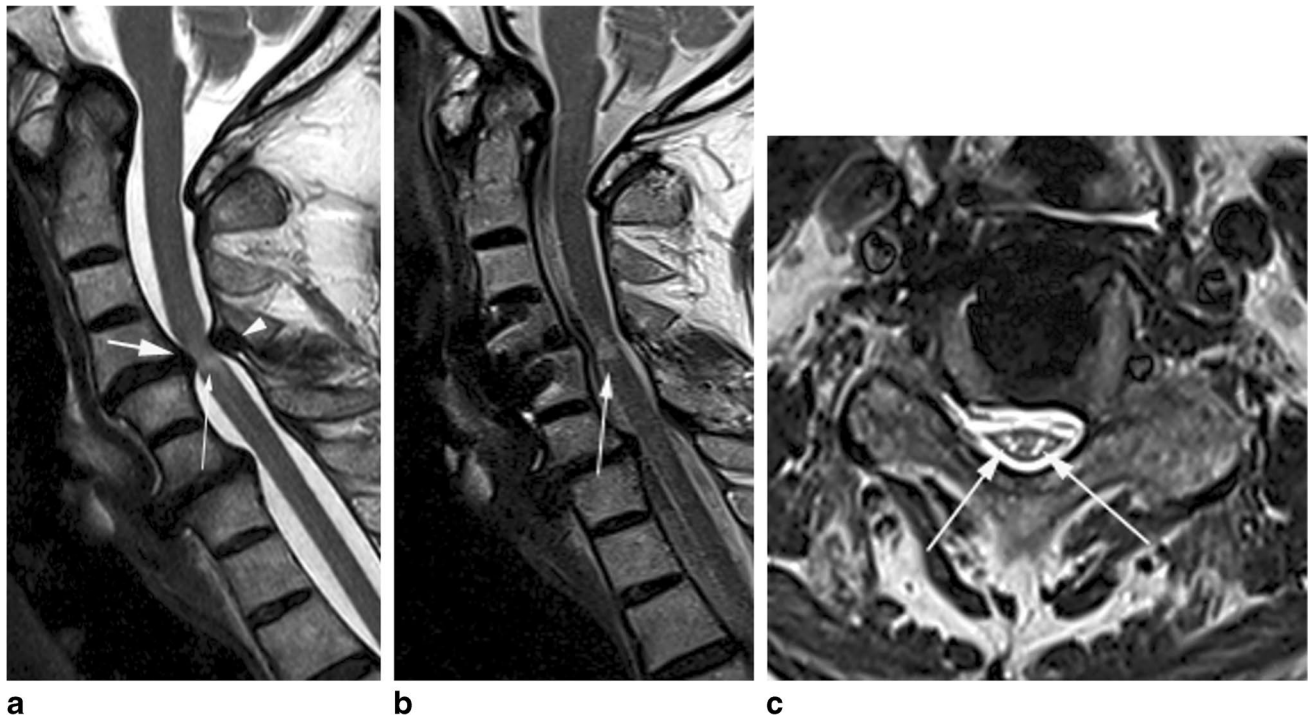
**Fig. 19** A 53-year-old male presenting with clinical features of myelopathy and a previous history of juvenile rheumatoid arthritis. (**a**) Sagittal T2W FSE MR image showing a degenerate bulging C4-C5 disc (arrow) with associated ligamentum flavum thickening (arrowhead) resulting in cord compression and myelomalacia (thin arrow). (**b**) T2W FSE MR image following C4-C5 ACDF showing residual myelomalacia and mild cord atrophy (thin arrow) despite adequate decompression. (**c**) Axial T2W FSE MR image showing the typical 'snake-eye' appearance (arrows). There was no post-operative clinical improvement

The association between reduced T1W SI and poor clinical outcome is supported by histological studies demonstrating the presence of necrosis, myelomalacia, and spongiform change in areas of T1W hypointensity, compared to the oedema seen in areas of isolated T2W hyperintensity. Persistent or worsening T2W SI abnormality following surgical decompression is generally felt to be a poor prognostic indicator for clinical improvement (Fig. 19) [17, 106]. The sagittal extent of T2W SI abnormality is also related to severity of impairment in CSM [12]. Myelomalacia is a term given to a process of atrophy and gliosis of the cord and tends to be irreversible, appearing on MRI as areas of central cystic degeneration, syrinx formation, or atrophy [107].

Mizuno et al. [108] assessed the clinical significance of a specific type of intramedullary T2W SI abnormality, termed the 'snake-eye appearance' (SEA). SEA refers to the presence of 2 small, round/oval, symmetrical areas of T2W signal hyperintensity within the cord on axial imaging, said to resemble the face of a snake (Fig. 19c). The authors found a significant difference in the clinical improvement of patients with SEA vs. non-SEA signal abnormality. Histologically, SEA was associated with cystic necrosis in the ventrolateral posterior column and significant neuronal loss in the anterior horn. The authors concluded that SEA is an unfavourable prognostic factor for the recovery of upper-limb weakness.

The presence of intramedullary gadolinium enhancement on MRI has been linked with poorer post-operative clinical outcomes [17] and may also aid in diagnosis. A flat band of enhancement, described as 'pancake-like', when at the site of or just caudal to the site of maximal stenosis suggests a diagnosis of spondylosis-related myelopathy and can persist for years following decompressive surgery. In patients with alternative myelopathic aetiologies and co-existing spondylosis, this type of enhancement is not present. This is a finding supported by other studies [9, 109, 110]. The presence of gadolinium enhancement is found in 7.3% of CSM patients undergoing decompression, being associated with worse clinical outcome. At 1-year follow-up, enhancement resolved in 60% of patients [110].

The presence of contrast enhancement in CSM may be misdiagnosed as a neoplastic or inflammatory condition. Wang et al. [111] describe 2 cases of CSM misdiagnosed as transverse myelitis. They stated that enhancement in CSM tends to be transverse and 'band-like' at or just below the level of maximal compression, short segment on sagittal imaging, and peripheral on axial imaging, and that the area of enhancement was within and smaller than the corresponding T2W SI abnormality. In contrast, inflammatory myelopathy is usually more extensive and ill defined.

## Advanced imaging techniques

Intramedullary SI changes on standard T1W and T2W sequences are considered to represent spinal cord injury (SCI), and therefore, surgery performed at this stage is to prevent deterioration. Ideally, surgery for CSM should be performed prior to the occurrence of T2W cord hyperintensity to optimise post-operative functional outcome [112]. Utilisation of advanced imaging techniques such as diffusion weighted imaging (DWI) [26], dynamic susceptibility contrast perfusion MRI [113], diffusion tensor imaging [114, 115, 116], MR spectroscopy (MRS) [117, 118, 119], and T1-mapping using an MP2RAGE [120] can provide information regarding microstructural integrity of the cord and cord ischaemia and can therefore aid in the selection of surgical candidates and in the prediction of post-operative outcomes. Detailed discussion of these techniques is outside the scope of this paper.

With regard DTI for CSM, Nischal et al. [121] undertook a prospective study of 52 patients suspected of CSM with different symptoms of myelopathy, graded as mild ($n = 11$), moderate ($n = 25$), and severe ($n = 16$). All patients underwent MRI of the cervical spine with DTI. At the most stenotic segments, the mean functional anisotropy (FA) value was significantly lower ($0.5009 \pm 0.087$ vs. $0.655.7 \pm 0.104$, $p < 0.001$), and the mean ADC value significantly higher ($1.196.5 \pm 0.311$ vs. $0.9370 \pm 0.284$, $p < 0.001$) than that in the non-stenotic segments. The sensitivity was better with FA (87.5%) and ADC (75.0%) than with T2W images (25%). The authors concluded that in addition to the routine MRI sequences, DTI metrics (FA value better than ADC) can detect myelopathy in patients with a clinically mild myelopathy grade before irreversible changes become apparent on routine T2W imaging and thus potentially enhance the outcome of decompression surgery.

Ellingson et al. [113] assessed the role of perfusion and ischaemia in the pathogenesis of CSM using spinal cord perfusion MRI. Twenty-two patients with cervical spondylosis with or without CSM underwent dynamic susceptibility contrast perfusion MRI using of a spin-and-gradient echo planar acquisition before, during, and following contrast injection. Estimation of relative spinal cord blood volume (rSCBV), the reversible relaxation rate ($R_2á$), and relative oxygen extraction fraction ($rOEF = R_2á/rSCBV$) was calculated at the site of compression and compared with AP spinal cord diameter and modified Japanese Orthopaedic Association score. rSCBV was linearly correlated with both AP cord diameter and mJOA. $R_2á$ was linearly correlated with mJOA but not cord diameter, whilst rOEF was correlated with both cord diameter mJOA. They concluded that the results indicate that spinal cord compression results in ischemia/hypoxia, with the degree of ischemia/hypoxia being proportional to the degree of neurological impairment.

Merali et al. [122] assessed the role of a deep learning model for the detection of spinal cord compression on MRI in patients undergoing surgery for CSM. The deep learning model achieved an overall area under the curve of 0.94, with sensitivity of 0.88 and specificity of 0.89. The authors suggested that the model could improve the interpretation of cervical spine MRI in this clinical setting.

## The atlantoaxial joint

The atlantoaxial joint (AAJ) should be considered as a separate unit when discussing the cervical spine due to its unique anatomical features. It is a pivot synovial joint devoid of an IVD and allows for rotation only. There are 3 associated synovial joints; a central atlanto-dens joint and two lateral atlantoaxial joints. In addition to sub-axial arthritis, the presence of any atlanto-dens and lateral AAJ arthritis should be ascertained when reporting cervical spine imaging.

Atlanto-dens osteoarthritis and subsequent hypertrophic changes of the atlanto-dental joint is a rare cause of CSM, although it may be found in up to 88% of those aged > 60 years [123]. The condition often results from instability at the AAJ, which leads to hypertrophy of surrounding tissues and can have a 'pseudotumour' appearance. Radiological signs include osseous spurs, reduction in joint space, and ossicle formation, as well as intraosseous

cysts and transverse ligament calcification [123, 124, 125] (Fig. 8).

Osteoarthritis of the lateral masses of C1-C2, also known as lateral AAJ osteoarthritis (AAOA), is often under-appreciated. Prevalence is 5% in the 6th decade and 18% in the 9th decade. AAOA typically affects females and is usually unilateral [126]. AAOA is not associated with myelopathy, nor upper limb radiculopathy. The lateral AAJs are innervated by the C2 ventral ramus and these patients present with upper cervical or occipital pain, which may radiate to the post-auricular region and be a cause of headaches. Pain is typically exacerbated by head rotation [127].

AAOA may be discovered radiographically on the open mouth odontoid view, on cross-sectional imaging, or bone scintigraphy. Diagnostic and therapeutic injection may be performed in this region, and in refractory cases, C1-C2 lateral masses fusion can be considered. This procedure is a safe and effective treatment option [127, 128, 129].

Whilst rare, congenital abnormalities of the AAJ such as atlas hypoplasia may result in canal narrowing and subsequent myelopathy. Atlas hypoplasia should be considered pathological when AP sagittal canal diameter is < 14 mm (normal canal diameter 16–25 mm). At < 10 mm, patients are usually myelopathic [130]. Atlas hypoplasia is treated with C1 laminectomy [131]. Ossification of the cruciate ligament of the atlas can also result in canal narrowing and myelopathy, with causative factors including calcium phosphate deposition disease, obesity, and ageing [125].

## Rare complications of cervical spondylosis

### Syringomyelia

There are reports of syringomyelia occurring secondary to cervical spondylosis, with obstruction to CSF flow generally thought to be the underlying cause. Both clinical and radiological improvement may be seen after decompression [132, 133]. Bhagavathula et al. [132] used cine MRI to demonstrate obstruction to CSF flow in the subarachnoid space at the level of spondylosis in a patient with syringomyelia. CSF flow was free both anterior and posterior to the spinal cord at the foramen magnum, and near complete resolution of the syrinx was demonstrated on MRI 3 months following decompressive laminectomy. Alternative pathogeneses have been postulated, including development of myelomalacia from instability causing micro-trauma which progresses to in syrinx formation and arachnoid adhesions from repetitive friction during neck movement [134].

## Vascular complications of cervical spondylosis

There have been rare reports of stroke caused by vertebral artery compression from osteophytes around the cervical spine. Nishikawa et al. (135) described 2 such cases of 'wake-up' stroke; one as a result of superior articular process osteophytes at C5 and the other as a result of bilateral uncovertebral osteophytes at C5-C6. Dynamic angiography confirmed aggravation of stenosis on neck movement in both cases.

## Conclusion

Cervical spondylosis is an exceptionally common finding in the older adult patient and can result in significant morbidity. Imaging is integral in diagnosis and in the identification of complications such as myelopathy or radiculopathy. Whilst radiographs and CT have a place in assessment, MRI is undeniably the imaging modality of choice. Both soft tissue and bony structures should be interrogated as both have the potential to result in significant neurological compromise. MRI has a use not only in the identification of myelopathy, but in the identification of features denoting potential poor surgical outcome and therefore preventing unnecessary surgery. As newer imaging techniques become mainstream, it is likely that the identification of such patients will improve. The use of intravenous gadolinium is not standard practise, but has shown promise in the identification of spondylotic myelopathy. Whilst several grading systems exist for vertebral canal and foraminal stenosis, some are limited by their reliance on non-standard imaging techniques. Nevertheless, the above-described grading systems by Kang, Kim, and Park have shown good reproducibility, inter-, and intra-observer reliability. Although not used in standard practise, SW-MRI may offer a more reliable and sensitive way of detecting osseous cervical foraminal stenosis. When reporting, it should be remembered that the cervical spine is a dynamic structure and significant findings may not be apparent on static images. As always, a combination of clinical and radiological assessment is crucial in the management of this complex condition.

# Appendix

**Table 1** CT cervical spine protocol from the authors' institution. Scan parameters

| Protocol name | Spine/c-spine RNOH |
|---|---|
| Scan type | Helical |
| Collimation | 64×0.625 |
| Slice thickness | 0.8 mm |
| Increment | -0.4 mm |
| Kv/mA | 120/modulated |
| Dose right index | 18 |
| Pitch and rotation time | 0.984<br>0.5 s |
| Scan field of view | Body – 50 cm |
| Display field of view | Evolving – pan and zoom to centre on vertebrae |
| Patient positioning | Supine head first |
| Scan coverage | Petrous ridge to T1 but depending on clinical information limited scans covering interested levels should be done where possible |
| Contrast and timing | None |
| Post-processing | 2/2 mm sagittal and coronal MPRs, 3D if requested |
| Archiving | PACS – survey, both axial series, MPRs, and dose report |

## Declarations

## References

1. Daffner RH. Radiologic evaluation of chronic neck pain. Am Fam Physician. 2010;82(8):959–64 (Available from: http://www.ncbi.nlm.nih.gov/pubmed/20949890).
2. Kim C-H, Hwang JM, Park J-S, Han S, Park D. Predictability of severity of disc degeneration and disc protrusion using horizontal displacement of cervical dynamic radiographs. Medicine (Baltimore). 2018;97(25):e11098 (Available from: https://journals.lww.com/00005792-201806220-00035).
3. Malcolm GP. Surgical disorders of the cervical spine: presentation and management of common disorders. J Neurol Neurosurg Psychiatry. 2002;73(Suppl 1):i34-41 (Available from: http://www.ncbi.nlm.nih.gov/pubmed/12185260).
4. Yi JS, Cha JG, Han JK, Kim H-J. Imaging of herniated discs of the cervical spine: inter-modality differences between 64-slice multidetector CT and 1.5-T MRI. Korean J Radiol. 2015;16(4):881–8 (Available from: http://www.ncbi.nlm.nih.gov/pubmed/26175589).
5. Green C, Butler J, Eustace S, Poynton A, O'Byrne JM. Imaging modalities for cervical spondylotic stenosis and myelopathy. Adv Orthop. 2012;2012:1–4 (Available from: http://www.hindawi.com/journals/aorth/2012/908324/).
6. Waly FJ, Abduljabbar FH, Fortin M, Nooh A, Weber M. Preoperative computed tomography myelography parameters as predictors of outcome in patients with degenerative cervical myelopathy: results of a systematic review. Glob spine J. 2017;7(6):521–8 (Available from: http://www.ncbi.nlm.nih.gov/pubmed/28894681).
7. Abdulkarim JA, Dhingsa RL, Finlay DB. Magnetic resonance imaging of the cervical spine: frequency of degenerative changes in the intervertebral disc with relation to age. Clin Radiol. 2003;58(12):980–4 (Available from: https://linkinghub.elsevier.com/retrieve/pii/S0009926003002551).
8. Talekar K, Poplawski M, Hegde R, Cox M, Flanders A. Imaging of spinal cord injury: acute cervical spinal cord injury, cervical spondylotic myelopathy, and cord herniation. Semin Ultrasound, CT MRI. 2016;37(5):431–47 (Available from: https://linkinghub.elsevier.com/retrieve/pii/S0887217116300269).
9. Pessini Ferreira LM, Auger C, Kortazar Zubizarreta I, Gonzalez Chinchon G, Herrera I, Pla A, et al. MRI findings in cervical spondylotic myelopathy with gadolinium enhancement: review of seven cases. BJR Case Rep. 2021;7(2):20200133 (Available from: http://www.ncbi.nlm.nih.gov/pubmed/33841903).
10. Steilen D, Hauser R, Woldin B, Sawyer S. Chronic neck pain: making the connection between capsular ligament laxity and cervical instability. Open Orthop J. 2014;8:326–45 (Available from: http://www.ncbi.nlm.nih.gov/pubmed/25328557).
11. Fakhoury J, Dowling TJ. Cervical degenerative disc disease. StatPearls Publishing; 2022. (Available from: http://www.ncbi.nlm.nih.gov/pubmed/32809607).
12. Nouri A, Martin AR, Mikulis D, Fehlings MG. Magnetic resonance imaging assessment of degenerative cervical myelopathy: a review of structural changes and measurement techniques. Neurosurg Focus. 2016;40(6):E5 (Available from: https://thejns.org/view/journals/neurosurg-focus/40/6/article-pE5.xml).
13. Kushchayev SV, Glushko T, Jarraya M, Schuleri KH, Preul MC, Brooks ML, et al. ABCs of the degenerative spine. Insights Imaging. 2018;9(2):253–74 (Available from: https://insightsimaging.springeropen.com/articles/10.1007/s13244-017-0584-z).
14. Patel PD, Arutyunyan G, Plusch K, Vaccaro A Jr, Vaccaro AR. A review of cervical spine alignment in the normal and

degenerative spine. J spine Surg (Hong Kong). 2020;6(1):106–23 (Available from: https://pubmed.ncbi.nlm.nih.gov/32309650).

15. Bakhsheshian J, Mehta VA, Liu JC. Current diagnosis and management of cervical spondylotic myelopathy. Glob spine J. 2017;7(6):572–86 (Available from: https://pubmed.ncbi.nlm.nih.gov/28894688).

16. Alizada M, Li RR, Hayatullah G. Cervical instability in cervical spondylosis patients : significance of the radiographic index method for evaluation TT - Zervikale Instabilität bei Patienten mit Zervikalspondylose : Bedeutung der radiographischen Indexmethode für die Evaluierung. Orthopade. 2018;47(12):977–85 (Available from: https://pubmed.ncbi.nlm.nih.gov/30255359).

17. Toledano M, Bartleson JD. Cervical spondylotic myelopathy. Neurol Clin. 2013;31(1):287–305.

18. Strine TW, Hootman JM. US national prevalence and correlates of low back and neck pain among adults. Arthritis Rheum. 2007;57(4):656–65 (Available from: https://onlinelibrary.wiley.com/doi/10.1002/art.22684).

19. Binder AI. Cervical spondylosis and neck pain. BMJ. 2007;334(7592):527–31 (Available from: https://pubmed.ncbi.nlm.nih.gov/17347239).

20. Young WF. Cervical spondylotic myelopathy: a common cause of spinal cord dysfunction in older persons. Am Fam Physician. 2000;62(5):1064–70 (1073. Available from: http://www.ncbi.nlm.nih.gov/pubmed/10997531).

21. Wang C, Tian F, Zhou Y, He W, Cai Z. The incidence of cervical spondylosis decreases with aging in the elderly, and increases with aging in the young and adult population: a hospital-based clinical analysis. Clin Interv Aging. 2016;11:47–53 (Available from: http://www.ncbi.nlm.nih.gov/pubmed/26834465).

22. Abdalkader M, Guermazi A, Engebretsen L, Roemer FW, Jarraya M, Hayashi D, et al. MRI-detected spinal disc degenerative changes in athletes participating in the Rio de Janeiro 2016 Summer Olympics games. BMC Musculoskelet Disord. 2020;21(1):45 (Available from: https://bmcmusculoskeletdisord.biomedcentral.com/articles/10.1186/s12891-020-3057-3).

23. Jiang S-D, Jiang L-S, Dai L-Y. Degenerative cervical spondylolisthesis: a systematic review. Int Orthop. 2011;35(6):869–75 (Available from: http://link.springer.com/10.1007/s00264-010-1203-5).

24. de Oliveira Vilaça C, Orsini M, Leite MAA, de Freitas MRG, Davidovich E, Fiorelli R, et al. Cervical spondylotic myelopathy: what the neurologist should know. Neurol Int. 2016;8(4):6330 (Available from: http://www.ncbi.nlm.nih.gov/pubmed/27994827).

25. Lannon M, Kachur E. Degenerative cervical myelopathy: clinical presentation, assessment, and natural history. J Clin Med. 2021;10(16):3626 (Available from: https://www.mdpi.com/2077-0383/10/16/3626).

26. Ellingson BM, Salamon N, Holly LT. Advances in MR imaging for cervical spondylotic myelopathy. Eur Spine J. 2015;24(Suppl 2):197–208 (Available from: https://pubmed.ncbi.nlm.nih.gov/23917647).

27. Lebl DR, Hughes A, Cammisa FP, O'Leary PF. Cervical spondylotic myelopathy: pathophysiology, clinical presentation, and treatment. HSS J ®. 2011;7(2):170–8 (Available from: http://journals.sagepub.com/doi/10.1007/s11420-011-9208-1).

28. Jha SC, Miyazaki M, Tsumura H. Kinetic change of spinal cord compression on flexion-extension magnetic resonance imaging in cervical spine. Clin Neurol Neurosurg. 2018;174:86–91 (Available from: https://linkinghub.elsevier.com/retrieve/pii/S0303846718303792).

29. Zeitoun D, El Hajj F, Sariali E, Catonné Y, Pascal-Moussellard H. Evaluation of spinal cord compression and hyperintense intramedullary lesions on T2-weighted sequences in patients with cervical spondylotic myelopathy using flexion-extension MRI protocol. Spine J. 2015;15(4):668–74 (Available from: https://linkinghub.elsevier.com/retrieve/pii/S152994301401771719).

30. Zeng C, Xiong J, Wang JC, Inoue H, Tan Y, Tian H, et al. The evaluation and observation of "hidden" hypertrophy of cervical ligamentum flavum, cervical canal, and related factors using kinetic magnetic resonance imaging. Glob spine J. 2016;6(2):155–63.

31. Sayıt E, Aghdasi B, Daubs MD, Wang JC. The occupancy of the components in the cervical spine and their changes with extension and flexion. Glob Spine J. 2015;5(5):396–405 (Available from: http://journals.sagepub.com/doi/10.1055/s-0035-1550089).

32. Lao L, Zhong G, Li Q, Liu Z. Kinetic magnetic resonance imaging analysis of spinal degeneration: a systematic review. Orthop Surg. 2014;6(4):294–9 (Available from: https://onlinelibrary.wiley.com/doi/10.1111/os.12137).

33. Xu N, Wang S, Yuan H, Liu X, Liu Z. Does dynamic supine magnetic resonance imaging improve the diagnostic accuracy of cervical spondylotic myelopathy? A review of the current evidence. World Neurosurg. 2017;100:474–9 (Available from: https://linkinghub.elsevier.com/retrieve/pii/S1878875017300700).

34. Xu N, Zhang Y, Zhou G, Zhao Q, Wang S. The value of dynamic MRI in the treatment of cervical spondylotic myelopathy: a protocol for a prospective randomized clinical trial. BMC Musculoskelet Disord. 2020;21(1):83 (Available from: https://bmcmusculoskeletdisord.biomedcentral.com/articles/10.1186/s12891-020-3106-y).

35. Ulbrich EJ, Schraner C, Boesch C, Hodler J, Busato A, Anderson SE, et al. Normative MR cervical spinal canal dimensions. Radiology. 2014;271(1):172–82 (Available from: http://pubs.rsna.org/doi/10.1148/radiol.13120370).

36. Murakami K, Nagata K, Hashizume H, Oka H, Muraki S, Ishimoto Y, et al. Prevalence of cervical anterior and posterior spondylolisthesis and its association with degenerative cervical myelopathy in a general population. Sci Rep. 2020;10(1):104 (Available from: http://www.nature.com/articles/s41598-020-67239-4).

37. Bajwa NS, Toy JO, Young EY, Ahn NU. Establishment of parameters for congenital stenosis of the cervical spine: an anatomic descriptive analysis of 1,066 cadaveric specimens. Eur Spine J. 2012;21(12):2467–74 (Available from: http://www.ncbi.nlm.nih.gov/pubmed/22829425).

38. Morishita Y, Naito M, Hymanson H, Miyazaki M, Wu G, Wang JC. The relationship between the cervical spinal canal diameter and the pathological changes in the cervical spine. Eur Spine J. 2009;18(6):877–83 (Available from: http://link.springer.com/10.1007/s00586-009-0968-y).

39. Nouri A, Tetreault L, Nori S, Martin AR, Nater A, Fehlings MG. Congenital cervical spine stenosis in a multicenter global cohort of patients with degenerative cervical myelopathy: an ambispective report based on a magnetic resonance imaging diagnostic criterion. Neurosurgery. 2018;83(3):521–8 (Available from: https://journals.lww.com/00006123-201809000-00025).

40. Yue W-M, Tan S-B, Tan M-H, Chi-Siong-Koh D, Tan C-T. The Torg-Pavlov ratio in cervical spondylotic myelopathy. Spine (Phila Pa 1976). 2001;26(16):1760–4 (Available from: http://journals.lww.com/00007632-200108150-00006).

41. Suk K-S, Kim K-T, Lee J-H, Lee S-H, Kim J-S, Kim J-Y. Reevaluation of the Pavlov ratio in patients with cervical myelopathy. Clin Orthop Surg. 2009;1(1):6 (Available from: https://ecios.org/DOIx.php?id=10.4055/cios.2009.1.1.6).

42. Prasad SS, O'Malley M, Caplan M, Shackleford IM, Pydisetty RK. MRI measurements of the cervical spine and their correlation to Pavlov's ratio. Spine (Phila Pa 1976). 2003;28(12):1263–8 (Available from: http://journals.lww.com/00007632-200306150-00009).

43. Kessler JT. Congenital narrowing of the cervical spinal canal. J Neurol Neurosurg Psychiatry. 1975;38(12):1218–24 (Available from: http://www.ncbi.nlm.nih.gov/pubmed/1219087).

44. Stratford J. Congenital cervical spinal stenosis a factor in myelopathy. Acta Neurochir (Wien). 1978;41(1–3):101–6 (Available from: http://link.springer.com/10.1007/BF01809140).

45. Zileli M, Borkar SA, Sinha S, Reinas R, Alves ÓL, Kim S-H, et al. Cervical spondylotic myelopathy: natural course and the value of diagnostic techniques –WFNS Spine Committee Recommendations. Neurospine. 2019;16(3):386–402 (Available from: http://e-neurospine.org/journal/view.php?doi=10.14245/ns.1938240.120).

46. Kang Y, Lee JW, Koh YH, Hur S, Kim SJ, Chai JW, et al. New MRI grading system for the cervical canal stenosis. AJR Am J Roentgenol. 2011;197(1):W134–40.

47. Waheed H, Khan MS, Muneeb A, Jahanzeb S, Ahmad MN. Radiologic assessment of cervical canal stenosis using Kang MRI Grading System: do clinical symptoms correlate with imaging findings? Cureus. 2019;11(7):e5073–e5073 (Available from: https://pubmed.ncbi.nlm.nih.gov/31511807).

48. Jiang S-D, Jiang L-S, Dai L-Y. Degenerative cervical spondylolisthesis: a systematic review. Int Orthop. 2011;35(6):869–75 (Available from: http://www.ncbi.nlm.nih.gov/pubmed/21264670).

49. Lee C, Woodring JH, Rogers LF, Kim KS. The radiographic distinction of degenerative slippage (spondylolisthesis and retrolisthesis) from traumatic slippage of the cervical spine. Skeletal Radiol. 1986;15(6):439–43 (Available from: http://link.springer.com/10.1007/BF00355101).

50. Dean CL, Gabriel JP, Cassinelli EH, Bolesta MJ, Bohlman HH. Degenerative spondylolisthesis of the cervical spine: analysis of 58 patients treated with anterior cervical decompression and fusion. Spine J. 2009;9(6):439–46 (Available from: https://linkinghub.elsevier.com/retrieve/pii/S1529943008014332).

51. Kawasaki M, Tani T, Ushida T, Ishida K. Anterolisthesis and retrolisthesis of the cervical spine in cervical spondylotic myelopathy in the elderly. J Orthop Sci. 2007;12(3):207–13 (Available from: https://linkinghub.elsevier.com/retrieve/pii/S0949265815323988).

52. Alvarez AP, Anderson A, Farhan S-D, Lu Y, Lee Y-P, Oh M, et al. The utility of flexion-extension radiographs in degenerative cervical spondylolisthesis. Clin Spine Surg. 2022;35(7):319–22 (Available from: https://journals.lww.com/10.1097/BSD.0000000000001307).

53. Tani T, Kawasaki M, Taniguchi S, Ushida T. Functional importance of degenerative spondylolisthesis in cervical spondylotic myelopathy in the elderly. Spine (Phila Pa 1976). 2003;28(11):1128–34 (Available from: http://www.ncbi.nlm.nih.gov/pubmed/12782980).

54. Gondar R, Nouri A, Jannelli G, Schaller K, Tessitore E. Does spondylolisthesis affect severity and outcome of degenerative cervical myelopathy? A systematic review and meta-analysis. Glob spine J. 2021;11(7):1134–41 (Available from: http://www.ncbi.nlm.nih.gov/pubmed/33063537).

55. Gondar R, Nouri A, Jannelli G, Schaller K, Tessitore E. Does spondylolisthesis affect severity and outcome of degenerative cervical myelopathy? A systematic review and meta-analysis. Glob Spine J. 2021;11(7):1134–41 (Available from: http://journals.sagepub.com/doi/10.1177/2192568220960452).

56. Bajamal AH, Kim S-H, Arifianto MR, Faris M, Subagio EA, Roitberg B, et al. Posterior surgical techniques for cervical spondylotic myelopathy: WFNS spine committee recommendations. Neurospine. 2019;16(3):421–34 (Available from: http://www.ncbi.nlm.nih.gov/pubmed/31607074).

57. Yalamanchili PK, Vives MJ, Chaudhary SB. Cervical spondylotic myelopathy: factors in choosing the surgical approach. Adv Orthop. 2012;2012:1–6 (Available from: http://www.hindawi.com/journals/aorth/2012/783762/).

58. Kim SW, Jang SB, Lee HM, Lee JH, Lee MU, Kim JW, et al. Analysis of cervical spine alignment and its relationship with other spinopelvic parameters after laminoplasty in patients with degenerative cervical myelopathy. J Clin Med. 2020;9(3):713 (Available from: http://www.ncbi.nlm.nih.gov/pubmed/32151098).

59. Shamji MF, Mohanty C, Massicotte EM, Fehlings MG. The association of cervical spine alignment with neurologic recovery in a prospective cohort of patients with surgical myelopathy: analysis of a series of 124 cases. World Neurosurg. 2016;86:112–9 (Available from: http://www.ncbi.nlm.nih.gov/pubmed/26409089).

60. Jeong H-W, Yi J, Lee S, Park S, Kang KN, Lee J, et al. Prognostic value of cervical ligamentum flavum thickness as a morphological parameter to predict cervical stenosis. Medicine (Baltimore). 2021;100(34):e27084–e27084 (Available from: https://pubmed.ncbi.nlm.nih.gov/34449510).

61. Abiola R, Rubery P, Mesfin A. Ossification of the posterior longitudinal ligament: etiology, diagnosis, and outcomes of nonoperative and operative management. Glob spine J. 2016;6(2):195–204.

62. Tetreault L, Nakashima H, Kato S, Kryshtalskyj M, Nagoshi N, Nouri A, et al. A systematic review of classification systems for cervical ossification of the posterior longitudinal ligament. Glob spine J. 2019;9(1):85–103 (Available from: https://pubmed.ncbi.nlm.nih.gov/30775213).

63. Ikegawa S. Genetics of ossification of the posterior longitudinal ligament of the spine: a mini review. J Bone Metab. 2014;21(2):127 (Available from: https://synapse.koreamed.org/DOIx.php?id=10.11005/jbm.2014.21.2.127).

64. Matsunaga S, Sakou T. OPLL: disease entity, incidence, literature search, and prognosis. In: OPLL. Tokyo: Springer Japan; 2006. p. 11–7 (Available from: http://link.springer.com/10.1007/978-4-431-32563-5_3).

65. Izumi T, Hirano T, Watanabe K, Sano A, Ito T, Endo N. Three-dimensional evaluation of volume change in ossification of the posterior longitudinal ligament of the cervical spine using computed tomography. Eur Spine J. 2013;22(11):2569–74 (Available from: http://www.ncbi.nlm.nih.gov/pubmed/24000076).

66. Wang H, Zou F, Jiang J, Lu F, Chen W, Ma X, et al. The correlation between ossification of the nuchal ligament and pathological changes of the cervical spine in patients with cervical spondylosis. Spine (Phila Pa 1976). 2014;39(26):B7-11 (Available from: http://www.ncbi.nlm.nih.gov/pubmed/25504097).

67. Eubanks JD. Cervical radiculopathy: nonoperative management of neck pain and radicular symptoms. Am Fam Physician. 2010;81(1):33–40 (Available from: http://www.ncbi.nlm.nih.gov/pubmed/20052961).

68. Caridi JM, Pumberger M, Hughes AP. Cervical radiculopathy: a review. HSS J. 2011;7(3):265–72 (Available from: http://www.ncbi.nlm.nih.gov/pubmed/23024624).

69. Taso M, Sommernes JH, Kolstad F, Sundseth J, Bjorland S, Pripp AH, et al. A randomised controlled trial comparing the effectiveness of surgical and nonsurgical treatment for cervical radiculopathy. BMC Musculoskelet Disord. 2020;21(1):171 (Available from: https://bmcmusculoskeletdisord.biomedcentral.com/articles/10.1186/s12891-020-3188-6).

70. Iyer S, Kim HJ. Cervical radiculopathy. Curr Rev Musculoskelet Med. 2016;9(3):272–80 (Available from: http://www.ncbi.nlm.nih.gov/pubmed/27250042).

71. Rhee JM, Yoon T, Riew KD. Cervical radiculopathy. J Am Acad Orthop Surg. 2007;15(8):486–94 (Available from: http://journals.lww.com/00124635-200708000-00005).

72. Nicotra A, Khalil NM, O'Neill K. Cervical radiculopathy: discrepancy or concordance between electromyography and magnetic

resonance imaging? Br J Neurosurg. 2011;25(6):789–90 (Available from: http://www.ncbi.nlm.nih.gov/pubmed/21899381).

73. Schroeder GD, Suleiman LI, Chioffe MA, Mangan JJ, McKenzie JC, Kepler CK, et al. The effect of oblique magnetic resonance imaging on surgical decision making for patients undergoing an anterior cervical discectomy and fusion for cervical radiculopathy. Int J spine Surg. 2019;13(3):302–7 (Available from: http://www.ncbi.nlm.nih.gov/pubmed/31328096).

74. Park MS, Moon S-H, Lee H-M, Kim T-H, Oh JK, Lee SY, et al. Diagnostic value of oblique magnetic resonance images for evaluating cervical foraminal stenosis. Spine J. 2015;15(4):607–11 (Available from: http://www.ncbi.nlm.nih.gov/pubmed/25452016).

75. Oshina M, Oshima Y, Tanaka S, Tan LA, Li XJ, Tuchman A, et al. Utility of oblique sagittal reformatted and three-dimensional surface reconstruction computed tomography in foraminal stenosis decompression. Sci Rep. 2018;8(1):16011 (Available from: http://www.ncbi.nlm.nih.gov/pubmed/30375504).

76. Schell A, Rhee JM, Holbrook J, Lenehan E, Park KY. Assessing foraminal stenosis in the cervical spine: a comparison of three-dimensional computed tomographic surface reconstruction to two-dimensional modalities. Glob spine J. 2017;7(3):266–71 (Available from: http://www.ncbi.nlm.nih.gov/pubmed/28660110).

77. Demondion X, Lefebvre G, Fisch O, Vandenbussche L, Cepparo J, Balbi V. Radiographic anatomy of the intervertebral cervical and lumbar foramina (vessels and variants). Diagn Interv Imaging. 2012;93(9):690–7 (Available from: https://www.sciencedirect.com/science/article/pii/S2211568412002811).

78. Park H-J, Kim SS, Lee S-Y, Park N-H, Chung E-C, Rho M-H, et al. A practical MRI grading system for cervical foraminal stenosis based on oblique sagittal images. Br J Radiol. 2013;86(1025):20120515 (Available from: https://pubmed.ncbi.nlm.nih.gov/23410800).

79. Park HJ, Kim SS, Han CH, Lee SY, Chung EC, Kim MS, et al. The clinical correlation of a new practical MRI method for grading cervical neural foraminal stenosis based on oblique sagittal images. AJR Am J Roentgenol. 2014;203(2):412–7.

80. Kim S, Lee JW, Chai JW, Yoo HJ, Kang Y, Seo J, et al. A new MRI grading system for cervical foraminal stenosis based on axial T2-weighted images. Korean J Radiol. 2015;16(6):1294–302.

81. Lee KH, Park HJ, Lee SY, Chung EC, Rho MH, Shin H, et al. Comparison of two MR grading systems for correlation between grade of cervical neural foraminal stenosis and clinical manifestations. Br J Radiol. 2016;89(1062):20150971 (Available from: https://pubmed.ncbi.nlm.nih.gov/27007709).

82. Meacock J, Schramm M, Selvanathan S, Currie S, Stocken D, Jayne D, et al. Systematic review of radiological cervical foraminal grading systems. Neuroradiology. 2021;63(3):305–16.

83. Engel G, Bender YY, Adams LC, Boker SM, Fahlenkamp UL, Wagner M, et al. Evaluation of osseous cervical foraminal stenosis in spinal radiculopathy using susceptibility-weighted magnetic resonance imaging. Eur Radiol. 2019;29(4):1855–62 (Available from: http://link.springer.com/10.1007/s00330-018-5769-4).

84. Argentieri EC, Koff MF, Breighner RE, Endo Y, Shah PH, Sneag DB. Diagnostic accuracy of zero-echo time MRI for the evaluation of cervical neural foraminal stenosis. Spine. 2018;43(13):928–33 (Available from: https://journals.lww.com/00007632-201807010-00016).

85. Lukies MW, Teoh WW, Clements W. Safety of CT-guided cervical nerve root corticosteroid injections. J Med Imaging Radiat Oncol. 2019;63(3):300–6 (Available from: http://www.ncbi.nlm.nih.gov/pubmed/30859711).

86. Desai A, Saha S, Sharma N, Huckerby L, Houghton R. The short- and medium-term effectiveness of CT-guided selective cervical nerve root injection for pain and disability. Skeletal Radiol. 2014;43(7):973–8 (Available from: http://www.ncbi.nlm.nih.gov/pubmed/24615407).

87. Kumaresan S, Yoganandan N, Pintar FA, Maiman DJ, Goel VK. Contribution of disc degeneration to osteophyte formation in the cervical spine: a biomechanical investigation. J Orthop Res. 2001;19(5):977–84 (Available from: http://doi.wiley.com/10.1016/S0736-0266%2801%2900010-9).

88. Papadopoulou S, Exarchakos G, Beris A, Ploumis A. Dysphagia associated with cervical spine and postural disorders. Dysphagia. 2013;28(4):469–80 (Available from: http://link.springer.com/10.1007/s00455-013-9484-7).

89. Yousem DM. Point: Don't call me a doc! Am J Neuroradiol. 2016;37(12):2180LP – 2180 (Available from: http://www.ajnr.org/content/37/12/2180.abstract).

90. Ross JS, editor. Counterpoint: appropriately ambiguous—the disc osteophyte complex. Am J Neuroradiol. 2016;37(12):2181–2181 (Available from: http://www.ajnr.org/content/37/12/2181.abstract).

91. Sengupta DK, Kirollos R, Findlay GF, Smith ET, Pearson JCG, Pigott T. The value of MR imaging in differentiating between hard and soft cervical disc disease: a comparison with intra-operative findings. Eur Spine J. 1999;8(3):199–204 (Available from: http://link.springer.com/10.1007/s005860050157).

92. Bender YY-N, Diederichs G, Walter TC, Wagner M, Liebig T, Rickert M, et al. Differentiation of osteophytes and disc herniations in spinal radiculopathy using susceptibility-weighted magnetic resonance imaging. Invest Radiol. 2017;52(2):75–80.

93. Ashana AO, Cohen JR, Evans B, Holly LT. Regression of anterior disk-osteophyte complex following cervical laminectomy and fusion for cervical spondylotic myelopathy. Clin spine Surg. 2017;30(5):E609-14 (Available from: http://www.ncbi.nlm.nih.gov/pubmed/28525486).

94. Mochida K, Komori H, Okawa A, Muneta T, Haro H, Shinomiya K. Regression of cervical disc herniation observed on magnetic resonance images. Spine (Phila Pa 1976). 1998;23(9):990–5 (Available from: http://journals.lww.com/00007632-199805010-00005).

95. Turk O, Yaldiz C. Spontaneous regression of cervical discs. Medicine (Baltimore). 2019;98(7):e14521 (Available from: https://journals.lww.com/00005792-201902150-00068).

96. Rahimizadeh A, Hassani V, Asgari N, Hamidifard M. Spontaneous regression of the sequestrated cervical discs: a prospective study of 70 cases. J Spine Neurosurg. 2018;07(01):e14521 (Available from: https://www.scitechnol.com/peer-review/spontaneous-regression-of-the-sequestrated-cervical-discs-a-prospective-study-of-70-cases-a7ms.php?article_id=7264).

97. Sharma AK, Gandhoke CS, Syal SK. Spontaneous regression of herniated cervical disc: a case report and literature review. Surg Neurol Int. 2021;12:141 (Available from: http://surgicalneurologyint.com/surgicalint-articles/spontaneous-regression-of-herniated-cervical-disc-a-case-report-and-literature-review/).

98. Rahimizadeh A, Hamidifard A SR. Spontaneous regression of the sequestrated cervical discs: a prospective study of 26 cases and review of the literature. World Spinal Column J. 2013;4:32–41.

99. Autio RA, Karppinen J, Niinimäki J, Ojala R, Kurunlahti M, Haapea M, et al. Determinants of spontaneous resorption of intervertebral disc herniations. Spine. 2006;31(11):1247–52 (Available from: http://journals.lww.com/00007632-200605150-00012).

100. Kobayashi N, Asamoto S, Doi H, Ikeda Y, Matusmoto K. Spontaneous regression of herniated cervical disc. Spine J. 2003;3(2):171–3 (Available from: https://linkinghub.elsevier.com/retrieve/pii/S1529943002005569).

101. Mummaneni PV, Kaiser MG, Matz PG, Anderson PA, Groff M, Heary R, et al. Preoperative patient selection with magnetic

resonance imaging, computed tomography, and electroencephalography: does the test predict outcome after cervical surgery? J Neurosurg Spine SPI. 2009;11(2):119–29 (Available from: https://thejns.org/spine/view/journals/j-neurosurg-spine/11/2/article-p119.xml).

102. Chen H, Pan J, Nisar M, Zeng HB, Dai LF, Lou C, et al. The value of preoperative magnetic resonance imaging in predicting postoperative recovery in patients with cervical spondylosis myelopathy: a meta-analysis. Clinics (Sao Paulo). 2016;71(3):179–84 (Available from: https://pubmed.ncbi.nlm.nih.gov/27074180).

103. Chikhale CB, Khurjekar KS, Shyam AK, Sancheti PK. Correlation between preoperative magnetic resonance imaging signal intensity changes and clinical outcomes in patients surgically treated for cervical myeloradiculopathy. Asian Spine J. 2017;11(2):174–80 (Available from: http://www.ncbi.nlm.nih.gov/pubmed/28443160).

104. Suri A, Chabbra RPS, Mehta VS, Gaikwad S, Pandey RM. Effect of intramedullary signal changes on the surgical outcome of patients with cervical spondylotic myelopathy. Spine J. 2003;3(1):33–45 (Available from: https://linkinghub.elsevier.com/retrieve/pii/S1529943002004485).

105. Mastronardi L, Elsawaf A, Roperto R, Bozzao A, Caroli M, Ferrante M, et al. Prognostic relevance of the postoperative evolution of intramedullary spinal cord changes in signal intensity on magnetic resonance imaging after anterior decompression for cervical spondylotic myelopathy. J Neurosurg Spine. 2007;7(6):615–22 (Available from: https://thejns.org/view/journals/j-neurosurg-spine/7/6/article-p615.xml).

106. Yagi M, Ninomiya K, Kihara M, Horiuchi Y. Long-term surgical outcome and risk factors in patients with cervical myelopathy and a change in signal intensity of intramedullary spinal cord on magnetic resonance imaging. J Neurosurg Spine. 2010;12(1):59–65 (Available from: https://thejns.org/view/journals/j-neurosurg-spine/12/1/article-p59.xml).

107. Ramanauskas WL, Wilner HI, Metes JJ, Lazo A, Kelly JK. MR imaging of compressive myelomalacia. J Comput Assist Tomogr. 1989;13(3):399–404 (Available from: http://journals.lww.com/00004728-198905000-00005).

108. Mizuno J, Nakagawa H, Inoue T, Hashizume Y. Clinicopathological study of "snake-eye appearance" in compressive myelopathy of the cervical spinal cord. J Neurosurg Spine. 2003;99(2):162–8 (Available from: https://thejns.org/view/journals/j-neurosurg-spine/99/2/article-p162.xml).

109. Flanagan EP, Krecke KN, Marsh RW, Giannini C, Keegan BM, Weinshenker BG. Specific pattern of gadolinium enhancement in spondylotic myelopathy. Ann Neurol. 2014;76(1):54–65.

110. Ozawa H, Sato T, Hyodo H, Ishii Y, Morozumi N, Koizumi Y, et al. Clinical significance of intramedullary Gd-DTPA enhancement in cervical myelopathy. Spinal Cord. 2010;48(5):415–22 (Available from: http://www.nature.com/articles/sc2009152).

111. Wang Y, Newsome SD. Cervical spondylotic myelopathy mimicking transverse myelitis. Mult Scler Relat Disord. 2019;31:131–3 (Available from: http://www.ncbi.nlm.nih.gov/pubmed/30986646).

112. Gembruch O, Jabbarli R, Rashidi A, Chihi M, Hetze S, Barthel L, et al. Surgery for degenerative cervical myelopathy. Spine (Phila Pa 1976). 2021;46(5):294–9 (Available from: https://journals.lww.com/10.1097/BRS.0000000000003750).

113. Ellingson BM, Woodworth DC, Leu K, Salamon N, Holly LT. Spinal cord perfusion MR imaging implicates both ischemia and hypoxia in the pathogenesis of cervical spondylosis. World Neurosurg. 2019;128:e773–81.

114. Shabani S, Kaushal M, Budde MD, Wang MC, Kurpad SN. Diffusion tensor imaging in cervical spondylotic myelopathy:

a review. J Neurosurg Spine. 2020:1–8. https://doi.org/10.3171/2019.12.SPINE191158.

115. Guan X, Fan G, Wu X, Gu G, Gu X, Zhang H, et al. Diffusion tensor imaging studies of cervical spondylotic myelopathy: a systemic review and meta-analysis. PLoS One. 2015;10(2):e0117707 (Available from: https://dx.plos.org/10.1371/journal.pone.0117707).

116. Rindler RS, Chokshi FH, Malcolm JG, Eshraghi SR, Mossa-Basha M, Chu JK, et al. Spinal diffusion tensor imaging in evaluation of preoperative and postoperative severity of cervical spondylotic myelopathy: systematic review of literature. World Neurosurg. 2017;99:150–8 (Available from: https://linkinghub.elsevier.com/retrieve/pii/S1878875016313006).

117. Zhang C, Das SK, Yang D-J, Yang H-F. Application of magnetic resonance imaging in cervical spondylotic myelopathy. World J Radiol. 2014;6(10):826–32 (Available from: https://pubmed.ncbi.nlm.nih.gov/25349665).

118. Uda T, Takami T, Tsuyuguchi N, Sakamoto S, Yamagata T, Ikeda H, et al. Assessment of cervical spondylotic myelopathy using diffusion tensor magnetic resonance imaging parameter at 3.0 tesla. Spine (Phila Pa 1976). 2013;38(5):407–14 (Available from: http://www.ncbi.nlm.nih.gov/pubmed/22914703).

119. Ellingson BM, Salamon N, Woodworth DC, Holly LT. Correlation between degree of subvoxel spinal cord compression measured with super-resolution tract density imaging and neurological impairment in cervical spondylotic myelopathy. J Neurosurg Spine. 2015;22(6):631–8 (Available from: http://www.ncbi.nlm.nih.gov/pubmed/25746116).

120. Baucher G, Rasoanandrianina H, Levy S, Pini L, Troude L, Roche P-H, et al. T1 mapping for microstructural assessment of the cervical spinal cord in the evaluation of patients with degenerative cervical myelopathy. Am J Neuroradiol. 2021;42(7):1348–57 (Available from: http://www.ajnr.org/lookup/doi/10.3174/ajnr.A7157).

121. Nischal N, Tripathi S, Singh JP. Quantitative evaluation of the diffusion tensor imaging matrix parameters and the subsequent correlation with the clinical assessment of disease severity in cervical spondylotic myelopathy. Asian Spine J. 2021;15(6):808–16 (Available from: http://www.ncbi.nlm.nih.gov/pubmed/33189108).

122. Merali Z, Wang JZ, Badhiwala JH, Witiw CD, Wilson JR, Fehlings MG. A deep learning model for detection of cervical spinal cord compression in MRI scans. Sci Rep. 2021;11(1):10473 (Available from: http://www.ncbi.nlm.nih.gov/pubmed/34006910).

123. Genez BM, Willis JJ, Lowrey CE, Lauerman WC, Woodruff W, Diaz MJ, et al. CT findings of degenerative arthritis of the atlantoodontoid joint. Am J Roentgenol. 1990;154(2):315–8 (Available from: http://www.ajronline.org/doi/10.2214/ajr.154.2.2105022).

124. Eren S, Kantarci M, Deniz O. Atlantodental osteoarthritis as a cause of upper cervical myelopathy: a case report. Eurasian J Med. 2008;40(3):137–9 (Available from: http://www.ncbi.nlm.nih.gov/pubmed/25610048).

125. Baqai MWS, Javed G, Baig MZ. Ossification of the cruciform ligament of atlas; a rare cause of cervical myelopathy: case report and review of literature. Asian J Neurosurg. 2019;14(3):999–1003 (Available from: http://www.ncbi.nlm.nih.gov/pubmed/31497151).

126. Schaeren S, Jeanneret B. Atlantoaxial osteoarthritis: case series and review of the literature. Eur Spine J. 2005;14(5):501–6 (Available from: http://link.springer.com/10.1007/s00586-004-0856-4).

127. Aprill C, Axinn M, Bogduk N. Occipital headaches stemming from the lateral atlanto-axial (C1–2) joint. Cephalalgia. 2002;22(1):15–22 (Available from: http://journals.sagepub.com/doi/10.1046/j.1468-2982.2002.00293.x).

128. Buraimoh MA, Massie LW, Montgomery DM. Lateral atlanto-axial osteoarthritis: a narrative literature review. Clin spine Surg. 2017;30(10):433–8.

129. Elliott RE, Tanweer O, Smith ML, Frempong-Boadu A. Outcomes of fusion for lateral atlantoaxial osteoarthritis: meta-analysis and review of literature. World Neurosurg. 2013;80(6):e337–46.

130. Hsu Y-H, Huang W-C, Liou K-D, Shih Y-H, Lee L-S, Cheng H. Cervical spinal stenosis and myelopathy due to atlas hypoplasia. J Chinese Med Assoc. 2007;70(8):339–44 (Available from: https://journals.lww.com/02118582-200708000-00006).

131. Pereira Duarte M, Camino Willhuber G, Petracchi M, Gruenberg M, Sola CA. Symptomatic atlas hypoplasia in a Latin-American patient: case report and literature review. J Am Acad Orthop Surg Glob Res Rev. 2021;5(5):e21.00041 (Available from: http://www.ncbi.nlm.nih.gov/pubmed/33945518).

132. Bhagavathula Venkata SS, Arimappamagan A, Lafazanos S, Pruthi N. Syringomyelia secondary to cervical spondylosis: case report and review of literature. J Neurosci Rural Pract. 2014;5(Suppl 1):S78-82 (Available from: http://www.ncbi.nlm.nih.gov/pubmed/25540552).

133. Athanasiou A, Magras I. Syringomyelia resolution after anterior cervical discectomy: a case report and literature review. Surg Neurol Int. 2019;10:42 (Available from: http://www.ncbi.nlm.nih.gov/pubmed/31528380).

134. Landi A, Nigro L, Marotta N, Mancarella C, Donnarumma P, Delfini R. Syringomyelia associated with cervical spondylosis: a rare condition. World J Clin cases. 2013;1(3):111–5 (Available from: http://www.ncbi.nlm.nih.gov/pubmed/24303479).

135. Nishikawa H, Miya F, Kitano Y, Mori G, Shimizu S, Suzuki H. Positional occlusion of vertebral artery due to cervical spondylosis as rare cause of wake-up stroke: report of two cases. World Neurosurg. 2017;98:877.e13-877.e21.